STAT

OSA - 2556-64
Cy 4 of 4

8-976

PROJECT 522 - TASK V

MEASUREMENT OF VHF TRANSMISSION AND REFLECTION IN A PLASMA

Final Report

May 5, 1964

STAT

TABLE OF CONTENTS

I. INTRODUCTION

This is the final report on the Measurement of VHF Transmission and Reflection in a Plasma started in September 1963 and completed in April 1964. The work described herein has also been referred to as The 20 KV Experiment and Task V of Project 522.

The work was undertaken in order to obtain experimental data on the basic characteristics of the ionized plasma cloud formed by injecting a high energy electron beam into a large volume of air at pressures in the range of 3 mm Hg to 20 mm Hg.

There were two general objectives to the plasma work - first, to derive the fundamental constants of the plasma from measurements of plasma growth and decay rate, electron density distribution, and production efficiency for various gas pressures and beam powers; and second, to obtain directly applicable performance data at 20 mm pressure as far as practicable with the 20 KV ionizing source.

In the category of basic constants we have determined approximate values for the recombination coefficient in nitrogen and air and the attachment coefficient in air. These will be useful in determining the characteristics of electron beam ionizing sources required to produce various sizes and shapes of plasma clouds. Experimental work was needed here because of the considerable spread in the values of basic constants appearing in the literature, especially for oxygen attachment, and the lack of data applying to the particular conditions of the application of interest here.

Another part of the work was concerned with the interaction of a 180 Mc electromagnetic wave with the plasma cloud in terms of reflection and attenuation effects. The experiments were carried out in a large rectangular waveguide in order to accurately control and measure the electromagnetic wave.

The 20 KV electron beams used as ionizing sources in this experiment have a range of only 10 inches in a gas at 20 mm pressure, and therefore the RF interaction data is limited in usefulness at this pressure, since the $\lambda_{\text{free space}}$ wave length at 180 Mc is about seven times the thickness of the plasma cloud and the effective propagation wavelength in the waveguide is still greater. The 20 KV energy level was chosen for the experiment, however, since 20 KV beam sources could be assembled quickly in the interests of speed in getting preliminary results.

The 20 KV experiment has served its purpose in generating preliminary values of the basic plasma constants, in determining some overall system performance characteristics at 20 mm pressure, particularly growth and decay time, and in demonstrating the usefulness of this kind of experiment for Project 522.

The Task V experiment has been disassembled and is now in the process of reassembly with a 150 KV, 3 to 5 kilowatt ionizing source capable of generating a 25 foot long plasma in the 21" x 42" waveguide at 20 mm gas pressure.

II. DESCRIPTION OF EQUIPMENT

A. General

The experiment is shown in schematic form in Fig. 1. The waveguide is a rectangular sealed aluminum tank 12 feet long with a 21 inch by 42 inch inside cross section. A TE_{10} electromagnetic wave at 180 Mc is launched into one end of the waveguide, and the plasma is formed at the other end by injection of two 20 KV electron beams. RF reflection effects are determined by measuring the magnitude and phase of the reflected wave observed at the sending end as deduced from voltage standing wave ratio (VSWR) and null position measurements made on the standing wave. RF attentuation measurements are made by measuring the change in RF voltage picked up by a loop near the plasma end of the waveguide as the plasma density is varied.

The experiment was originally designed for 3 mm gas pressure, and for this reason two electron guns were used in order to produce uniform filling of the waveguide with plasma. The work was later extended to higher gas pressures where the filling is far from uniform but where significant data on growth and decay rates of electron density can still be made.

The electron guns are of the cold cathode "PEB" or plasma electron beam type as developed in this laboratory. The electron beams are formed in separate cylindrical chambers at a gas pressure of 10 microns. They are focused into a small beam which is directed through a 3/16" aperture into a short differentially pumped chamber at about 100-200μ pressure, and thence through another 3/16" diameter aperture into the main chamber, where they produce the ionized plasma cloud. The beam current entering the chamber is controlled by defocusing the beam at the apertures and by varying the gas pressure in the beam forming chamber. A range of beam currents from 10^{-5} to 10^{-2} amperes (0.2 watt to 200 watts) per gun was obtained in this way.

TOP VIEW

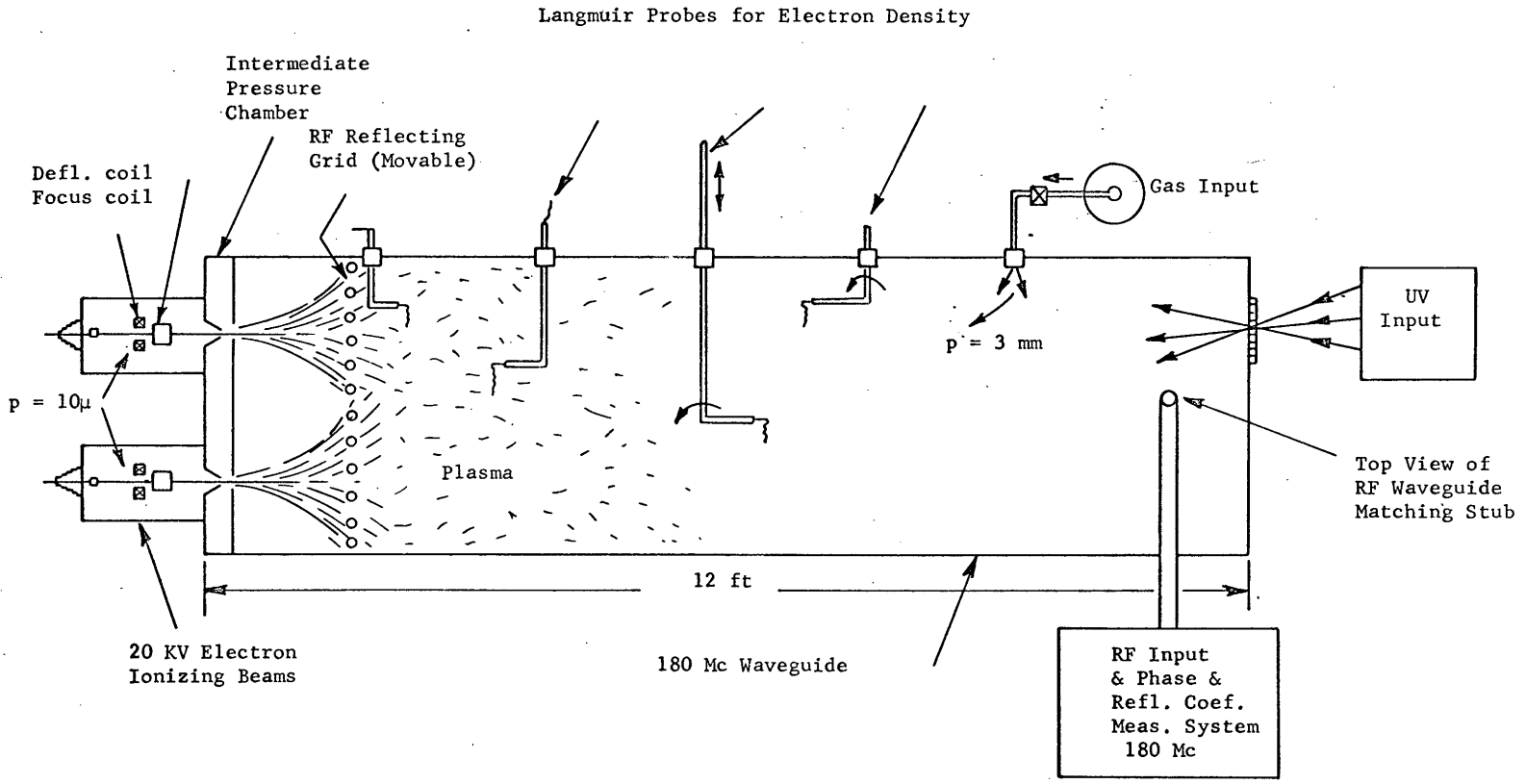

SCHEMATIC DIAGRAM OF OVERALL 20 KV EXPERIMENT

FIGURE #1

Transient excitation for observing plasma growth and decay characteristics is obtained by a fast acting magnetic deflection system which pulls the beam away from or onto the waveguide entrance apertures with a small fraction of a microsecond switching time.

Measurement of both steady state and transient beam current excitation is accomplished by current measuring cups which can be moved over the entrance apertures in the waveguide to collect the beam current. These measurements were checked calorimetrically with an agreement of about 10% between beam power as measured thermally and as the measured product of current and voltage.

B. Gas Control

The control of gas pressure in the waveguide is accomplished by varying the input gas flow rate. In general the intermediate chamber is pumped hard at a constant rate, so that its pressure is determined by the pressure in the main chamber and the size of the apertures. With two 3/16" diameter apertures the intermediate chamber pressure rises to about 1/2 mm when the main chamber pressure is adjusted to 20 mm. These are the highest pressures tolerable in the experiment with the pumping complement and apertures used, since above these pressures the diffusion booster pump used to control pressure in the beam forming chambers cannot reduce the pressure to the 10μ level required for the plasma electron beam cathode.

The gas flow, then, is from the bottled gas supply, through the waveguide, into the intermediate chamber and thence into the cathode chambers. The cathodes will operate equally well in an air or a pure nitrogen atmosphere.

The details of the gas pumping system were reported in the Project 522 - Task V Interim Technical Report for the period September - December 1963, and will not be further described here.

The gases used were either pure nitrogen or 80% nitrogen - 20% oxygen mixtures obtained in steel bottles from Olin Matheson Chemical Corp. The impurity content was listed by the vendor as follows:

Nitrogen

O_2----------5 - 10 ppm

H_2----------5 ppm

CO_2----------2 - 8 ppm

dew point ---------- 85° - 95°F

Oxygen

Ar ---------- 0.45%

H_2O ---------- 40 ppm

CH_4 ---------- 12 ppm

All others ---------- 1 ppm or less

Except for the relatively high Argon content in the oxygen, the gas impurity level in the gas supply was satisfactorily low.

In general the leak rate or outgassing rate of the system was checked before a run was made by pumping it all down to 1 micron pressure and observing the rate of rise of pressure. The leak rate was generally about 3μ per minute, but we occasionally made runs with two or three times this value. The gas flow rate at 3 mm pressure was about 100 times greater than the best leak rate and proportionately less for higher leak rates. At 20 mm pressure the gas flow rates were 700 times greater than the average leak rate.

Thus we would estimate that the gases used were contaminated with about 1% of laboratory air at 3 mm pressure and 1/7% at 20 mm pressure.

Gas samples were taken from time to time and analyzed on a mass spectrometer. In general these analyses confirmed the above conclusions. One of the analyses showed the presence of 0.7% of various hydrocarbons, but this is in doubt, since it did not repeat on other occasions.

SCHEMATIC DIAGRAM OF VACUUM SYSTEM

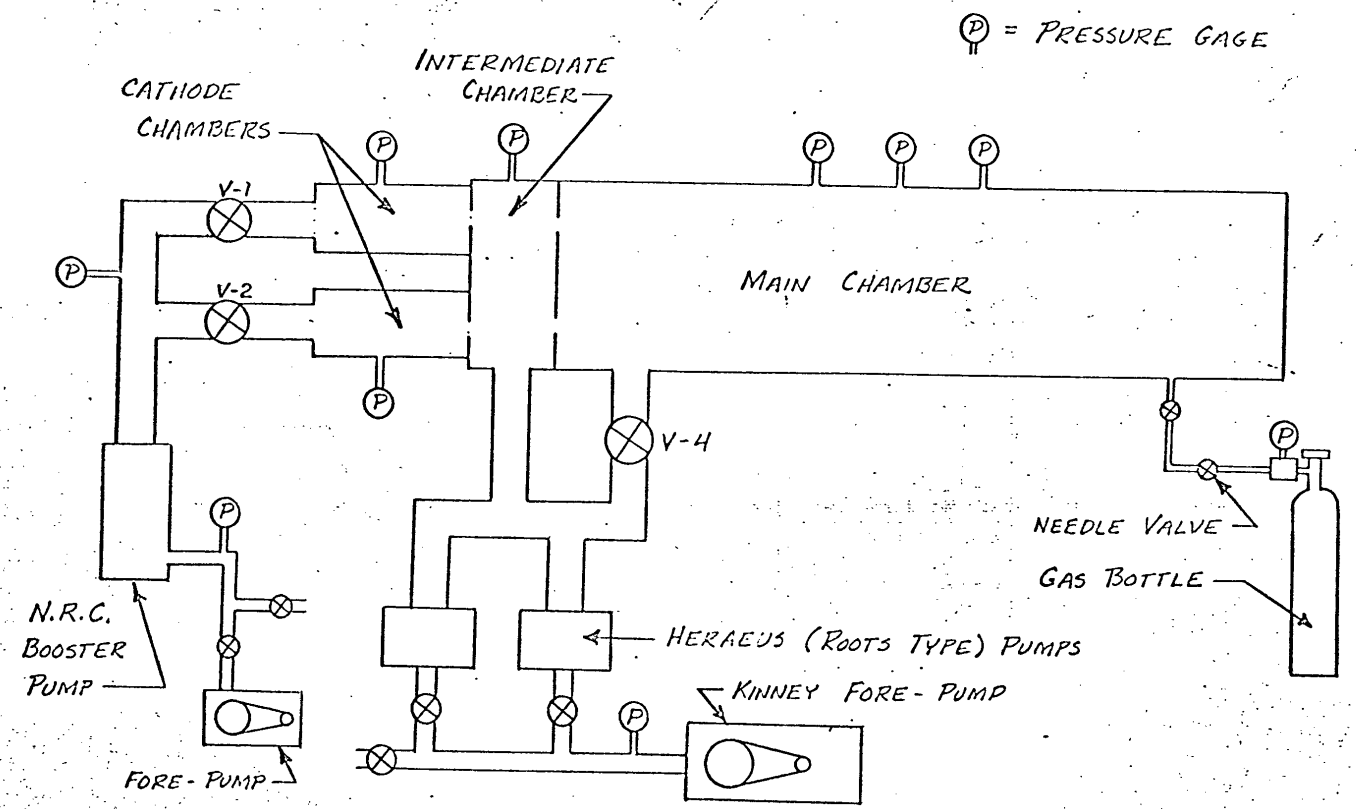

FIGURE 2

C. Electron Density Measurements

Electron density measurements in the plasma cloud were made using Langmuir probes introduced at various points along the waveguide as indicated in Fig. 1. The probes were generally 0.001" dia. by 3 cm long with the probe wire sealed into a long glass tube extending through a vacuum seal in the wave guide wall. The glass tubes were tapered down to a point in order to reduce plasma depletion by diffusion to the glass where the bare probe wire enters. The probe holders could be pushed into the chamber for varying distances so as to get transverse profiles of electron density.

Initially tungsten was used as the probe wire material, but tungsten proved to be unstable, and the wires acquired visible surface coatings after use in the air mixture which gave variable readings. Later, platinum plated tungsten was tried with some improvement. Iridium turned out to be the most stable probe wire material; it combines the inertness of platinum with greater rigidity.

Early probe measurements were made with an XY plotter using linear current vs voltage scales. Later, a logarithmic amplifier was introduced into the current measuring circuit, and the XY plots were produced directly on semi log paper. This simplified the data reduction process.

After discovering the stability difficulties, later readings were taken only after a short run-in period, and individual EI curves were repeated at the beginning and end of a run. In some cases the probe was heated by an initial period of high positive voltage, but this was of limited use in the air mixture where oxidation temperatures had to be avoided.

At the relatively high gas pressures we are concerned with, we do not find a clean break in the curve for location of plasma potential, but we used Langmuir's method of getting the plasma potential from the intercept of the I^2 vs V curve on the V axis for the high values of electron current. Electron temperature was derived

from the slope of the linear part of the log I vs E curve. An electron temperature in the order of 1200°K was observed under most conditions.

There were a number of cases observed in which the I^2 vs V curve did not come out linear and the plasma potential had to be more or less guessed at from the shape of the knee of the log I vs V curve. We did not discover the reason for this anomaly. In general it is felt that the probe measurements have an absolute accuracy of about $\pm$ 2 to 1, with a relative accuracy for profile measurements considerably better. A great many probe measurements were made at different times and with different probes for the same beam current and gas conditions, and the agreement was within the limits mentioned above except when some obvious anomaly occurred.

D. RF REFLECTION MEASURING SYSTEM

The RF measuring system is shown schematically in Fig. 3. It consists of a 50 milliwatt 180 Mc RF oscillator (General Radio "Unit Oscillator") feeding through a directional coupler and a type PRD-219 Standing Wave Indicator into a matching stub inserted in the waveguide. The matching stub excites a $TE_{1,0}$ mode in the waveguide which in combination with the wave reflected off the near end of the guide produces a traveling wave moving toward the plasma end of the guide. The wave reflected from the plasma or from the RF grid returns to the matching stub and produces a standing wave in the guide and in the VSWR indicator. The reflection coefficient is calculated from the measured VSWR, and the apparent reflection point from the measured phase shift of the standing wave null point.

The free space wavelength is 65.6 inches, and the cutoff wavelength is twice the long dimension of the guide, or 84 inches, so that waves having a wavelength longer than 84 inches cannot propagate in the guide, and are severely attenuated in a short distance.

Now the effect of a pure electron cloud without collisions is to decrease the dielectric constant of the medium and hence to increase the wavelength of electromagnetic waves propagating through it. In free space that value of electron density which reduces the dielectric constant to zero, corresponding to infinite wavelength and essentially zero propagation is the plasma resonant density at the frequency under consideration. In the waveguide, however, the wavelength need be increased only by a factor of 84 ÷ 65.5 to produce "waveguide cutoff", and the corresponding electron density required to produce waveguide cutoff is only about 0.4 of the free space plasma resonant density. The free space plasma resonant density, neglecting collisions, is $\sim 4 \times 10^8$/cc at 180 MC, while the waveguide cutoff density is only $\sim 1.6 \times 10^8$ electrons per cc.

The effect of electron collisions with gas molecules is to raise the "cutoff density" and to produce losses in transmission.

A typical value of collision frequency at 3 mm pressure and for 1200°K electron temperature is 10^9/sec. The angular frequency, w, at 180 Mc is 1.13×10^9/sec, so that for the 3 mm experiments the collision frequency, ν, is nearly equal to w and the plasma conductivity is nearly maximum. The electron density required for given plasma characteristics is increased above the collisionless value, both in free space and in the waveguide, by the factor $\left(1 + \frac{\nu^2}{w^2} \right)$. Accordingly, waveguide cutoff for this collision frequency will occur at a density of $\left(1 + \frac{1}{1.278}\right) \times 1.6 \times 10^8 = 2.8 \times 10^8$ electrons/cm^3.

An RF reflecting grid consisting of a metal frame contacting the top and bottom of the waveguide with spring fingers and enclosing a series of vertical wires parallel to the E field was used to provide an adjustable position reflection point for the RF wave. The RF grid was adjustable in position axially along the waveguide by four positioning rods controllable from outside the chamber, and was initially designed to provide a means of locating the RF reflection point at a distance from the injection end in the region where the plasma has become fairly uniform. During operation it also turned out to be useful in establishing that at high electron densities very little, if any, RF penetration reached as far as the grid, since in the high current region movement of the grid did not produce a corresponding movement of the null point of the standing wave. The RF shorting grid had a projected area of 10%, so that it removed only about 10% of the primary electrons and thus had a small effect on plasma production rate.

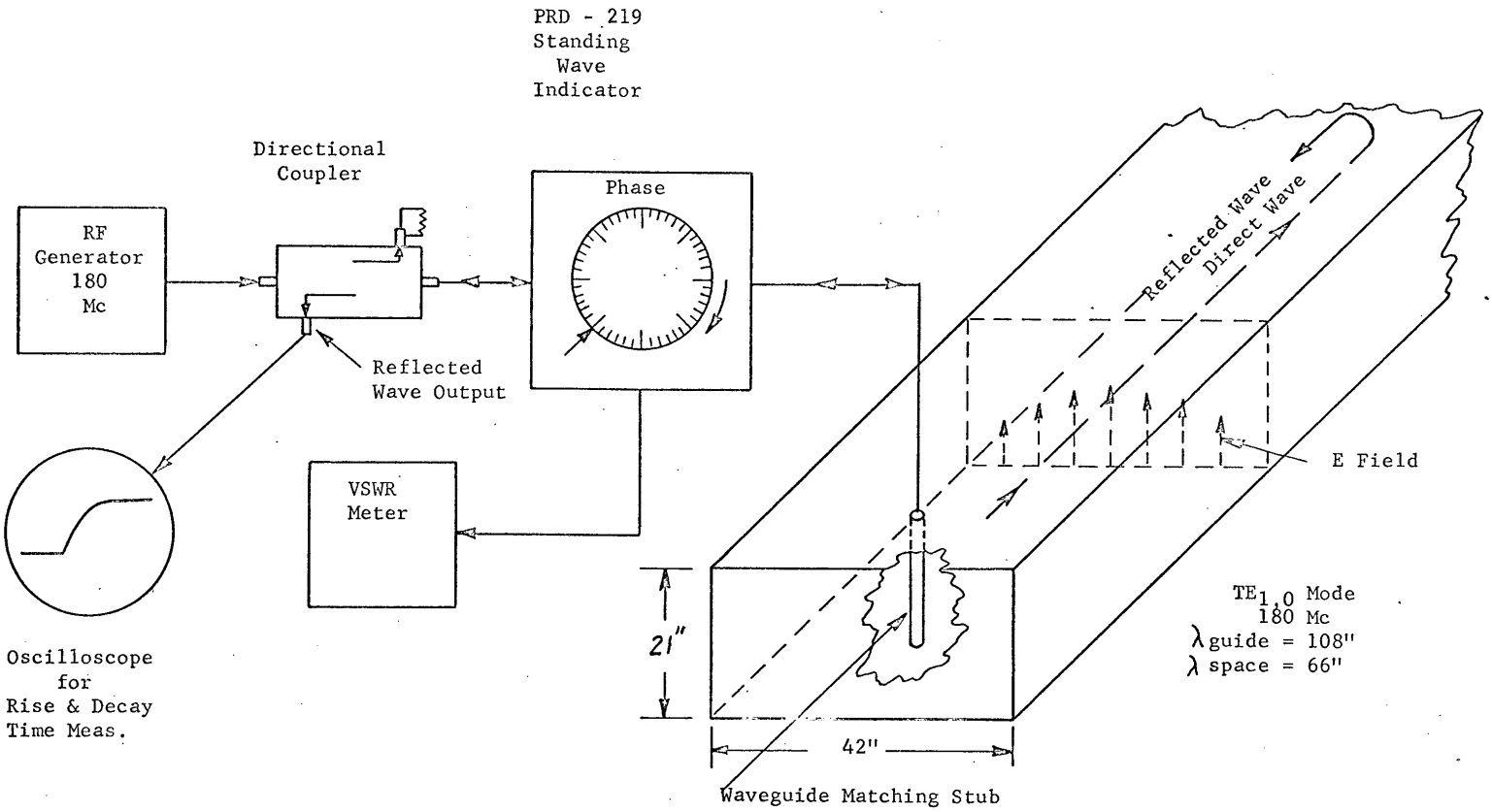

SCHEMATIC DIAGRAM OF RF REFLECTION MEASURING SYSTEM

FIGURE #3

III. EXPERIMENTAL RESULTS

A. Probe Measurements

Electron density profile measurements were made at one foot intervals along the central axis of the waveguide at various beam currents for both the pure nitrogen and the air mixture. The resulting electron density profiles are shown on Figures 4 & 5 for 3 mm gas pressure.

The profiles all show a characteristic shape with a peak in electron density at 2 or 3 feet from the beam injection plane and then a gradual taper downward at increasing distances from the apertures with a rapid cutoff at the end of the range at about 7 feet. The reduction in density near the injection aperture plane results from the trough between the two primary beams. Visual observations of the glowing plasma show that the primary beam scatters into a cone with an exponentially increasing diameter with a diameter of about 8" at 1 foot from the gun at 3 mm gas pressure. At three feet from the gun the two beams have merged and produced a uniform density across the cross section of the waveguide as shown in the transverse profile of Fig. 6.

The density profiles produced in air are equal within the experimental error to those produced in nitrogen except for the 20 microampere beam current profile, where the electron density in air is significantly lower than that in nitrogen. The difference is attributed to electron attachment processes in oxygen which produce a loss rate proportional to the electron density, whereas the recombination losses common to both oxygen and nitrogen are proportional to the square of the electron density. Thus at high density levels the recombination process dominates, and a given beam current produces equal electron densities in both the nitrogen and the air mixture. At lower densities, however, the loss rate is dominated by attachment loss in the air mixture so that very low beam currents produce less density in air than in nitrogen.

Diffusion losses are also proportional to the first power of electron density and therefore affect nitrogen and air equally. However, because of the large size of the waveguide the diffusion losses are negligible at the center of the waveguide, at least at the higher densities where recombination losses are high. For example, the zero gradient of density existing in the central region of the tank as in Fig. 6 for a 2 ma beam current shows that there is a minimum of diffusion loss at the center for that particular condition. There is some diffusion loss in the 8" diameter pipe described in the section on wall effects as shown in Figs. 25 and 26 . In that case it can also be seen that in the higher current condition, the 10 ma curve, diffusion has less effect than in the 1 ma curve, as would be expected.

Diffusion losses become more important at lower beam currents where other losses are less effective and are probably responsible for the apparent foreshortening of the axial profile or apparent reduction in range for the low beam currents as seen in Figures 4 & 5.

ELECTRON DENSITY PROFILES

FOR NITROGEN PLASMA

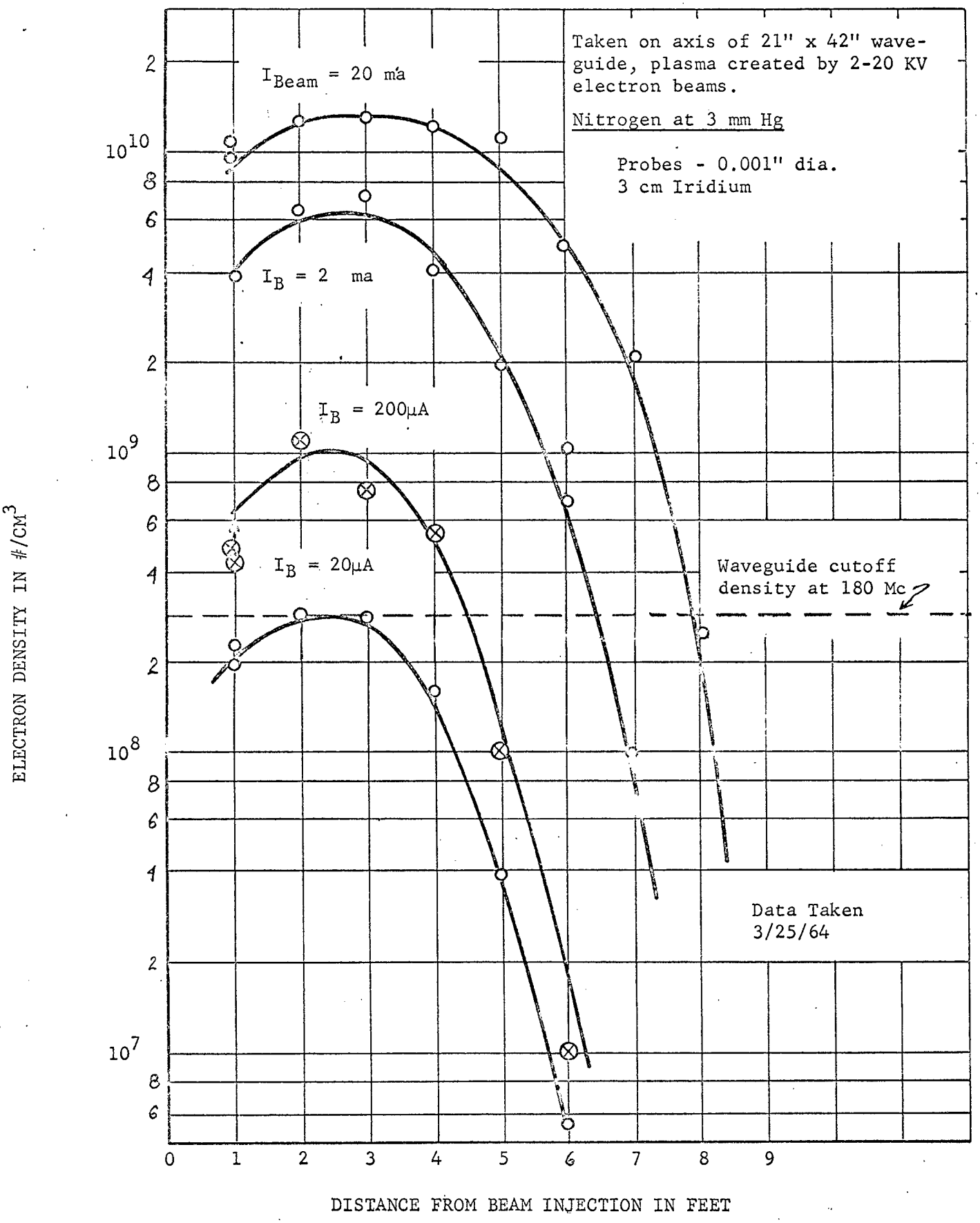

FIGURE #4

ELECTRON DENSITY PROFILES
FOR AIR PLASMA

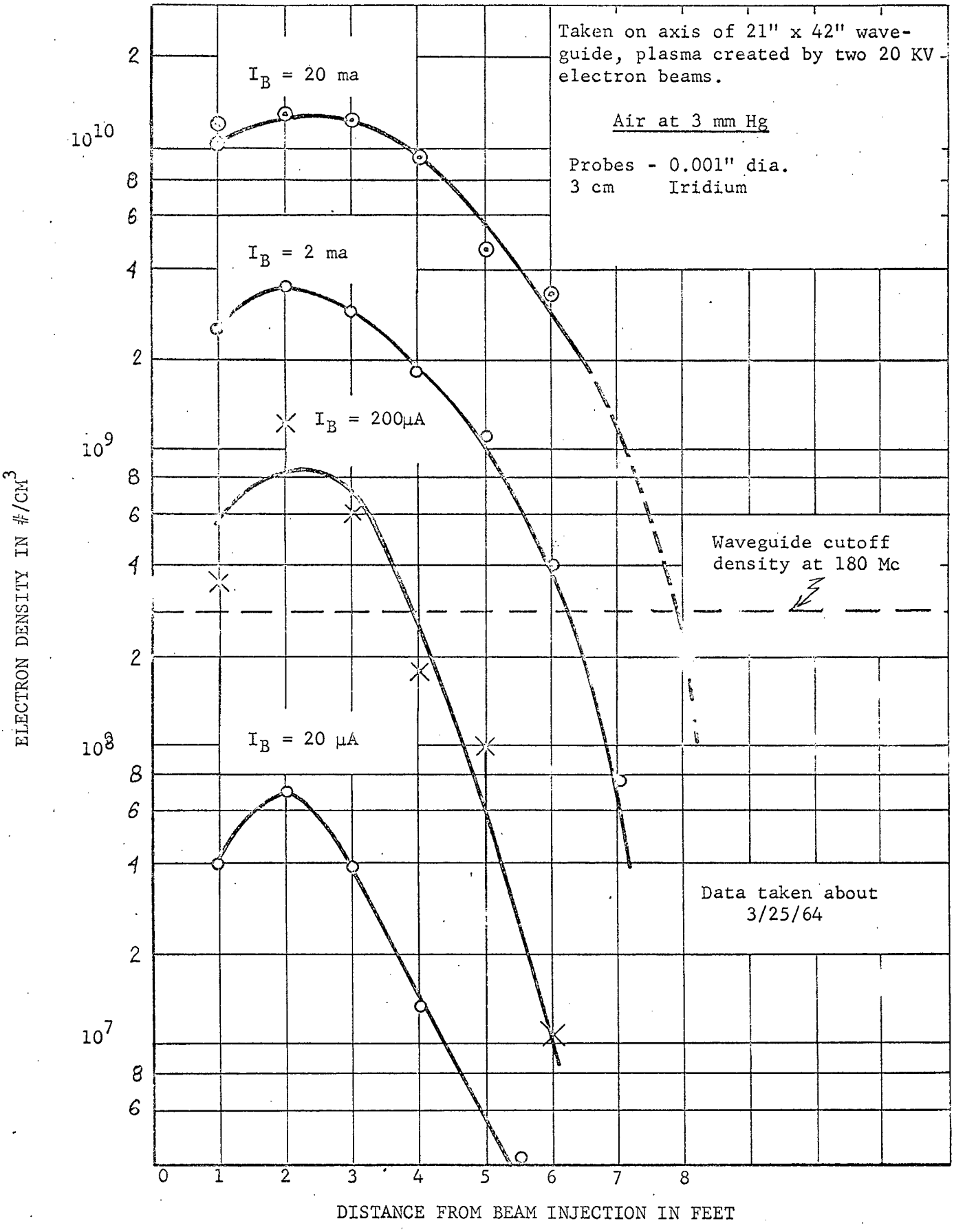

FIGURE 5

DISTRIBUTION OF ELECTRON DENSITY

ACROSS THE WAVEGUIDE

Nitrogen at 3 mm, 36" from Injection Plane
1/2 mil dia x 3 cm Iridium Probe

I_b = 2 ma, 20 KV

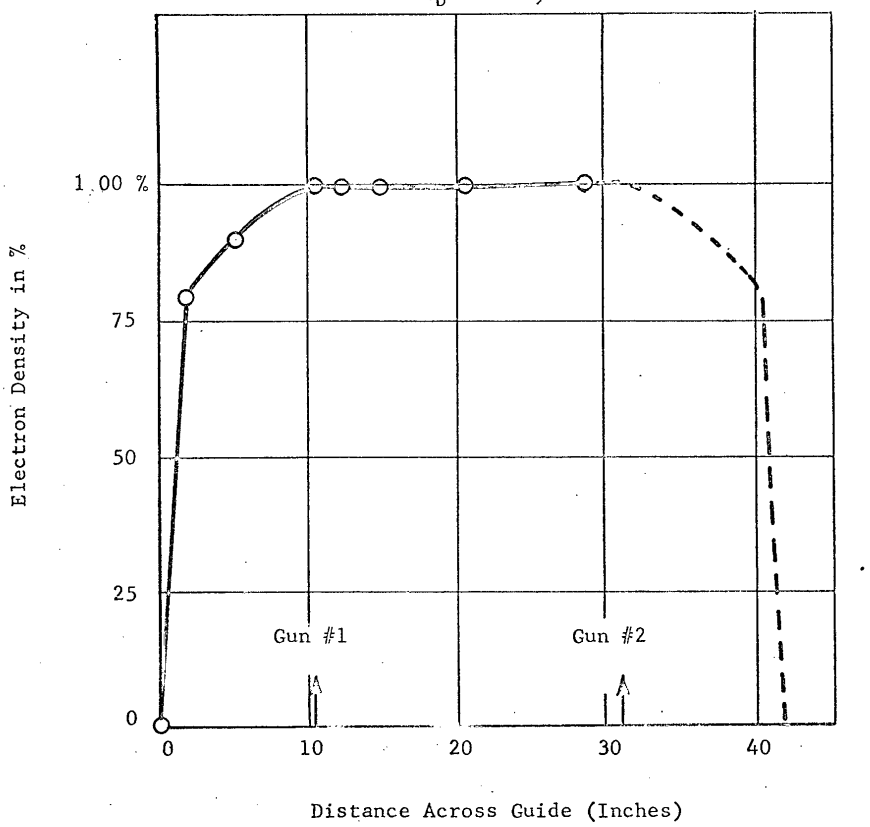

FIGURE #6

B. Steady State RF Reflection

Having determined the shape of the electron density profiles along the axis of the waveguide, we are now in a position to analyze the behavior of the electromagnetic wave which travels down the waveguide and encounters the plasma cloud.

In a preceeding section it was shown that for electron densities exceeding 2.8×10^8 per cm^3 the 180 Mc wave can no longer propogate as a plane wave because its wavelength in the waveguide is increased by the plasma beyond the cutoff wavelength of the guide. Thus for all densities above 2.8×10^3 per cm^3 the plane wave becomes an evanescent wave, it acquires field components axially along the waveguide, and its field strength diminishes very rapidly within the plasma.

If there were no collision losses and if the gradient were very long compared to a wavelength, the wave would be totally reflected. However, in the actual experiment there are collision losses and the density gradient does not occur over a distance large compared to a wavelength, so perfect reflection would not be expected. The mathematical analysis for this situation is quite complex and has not been attempted here; nevertheless it is instructive to analyze the RF behaviour qualitatively, since the experiment does show us the actual behaviour of the RF wave for the particular conditions existing in the waveguide. Furthermore, as described in a later section, it is believed that a valid extrapolation can be made from waveguide measurements to the free space situation.

We cannot extrapolate all the way from the 7 foot plasma at 3 mm pressure in a waveguide to a 25 foot plasma at 20 mm pressure in free space nor can we extrapolate from the very short 1 foot long plasma at 20 mm in the waveguide because the conditions are too dissimilar in too many respects. The extrapolation from the 25 foot plasma to be obtained at 20 mm pressure in the 150 KV experiment,

however, should not be so difficult.

Returning to the RF behaviour observed in the 20 KV experiment we have mentioned that above a density in the order of 2.8×10^8 per cm^3 we would expect but little penetration of the plasma; we would expect only moderate attenuation of the reflected wave, and we would expect the reflection point to occur near that part of the profile where the cut off density is first encountered by the wave.

If the whole of the plasma cloud were below the cut off density, we would expect maximum penetration as observed by the position of the null. Since the attenuation is proportional to the electron density in the propagating mode, we would expect minimum reflection to occur at that value of beam current which produces a maximum density just under the critical or cutoff density in the waveguide. At still lower densities the incident wave will continue to traverse the whole plasma as far as the RF reflecting grid and then will travel back out to the RF measuring end with an attenuation that decreases as beam current decreases.

Qualitatively, and within the variations which might be expected from the shortness of the plasma relative to a wavelength, the behaviour described above is what actually occurs. For example, considering the nitrogen plasma, inspection of the electron density profile in Figure 4 shows that cut off density is first reached at 20μA beam current. Thus we would expect maximum attenuation or minimum reflection to occur for a beam current somewhat above 20μA, since an appreciable thickness of the cloud must be present to produce reflection. Reference to the 3 mm curve in Figure 7 shows that the voltage reflection coefficient in fact decreases from the empty waveguide value of 90% or more as the beam current is gradually increased, and reaches a minimum value at a beam current of 40μ amps, as might be expected. Above 40μ amps, where the wave penetrates less and less of the plasma, the attenuation is gradually decreased and the reflection coefficient increases again, reaching a fairly constant value of about 60% for very overdense plasmas.

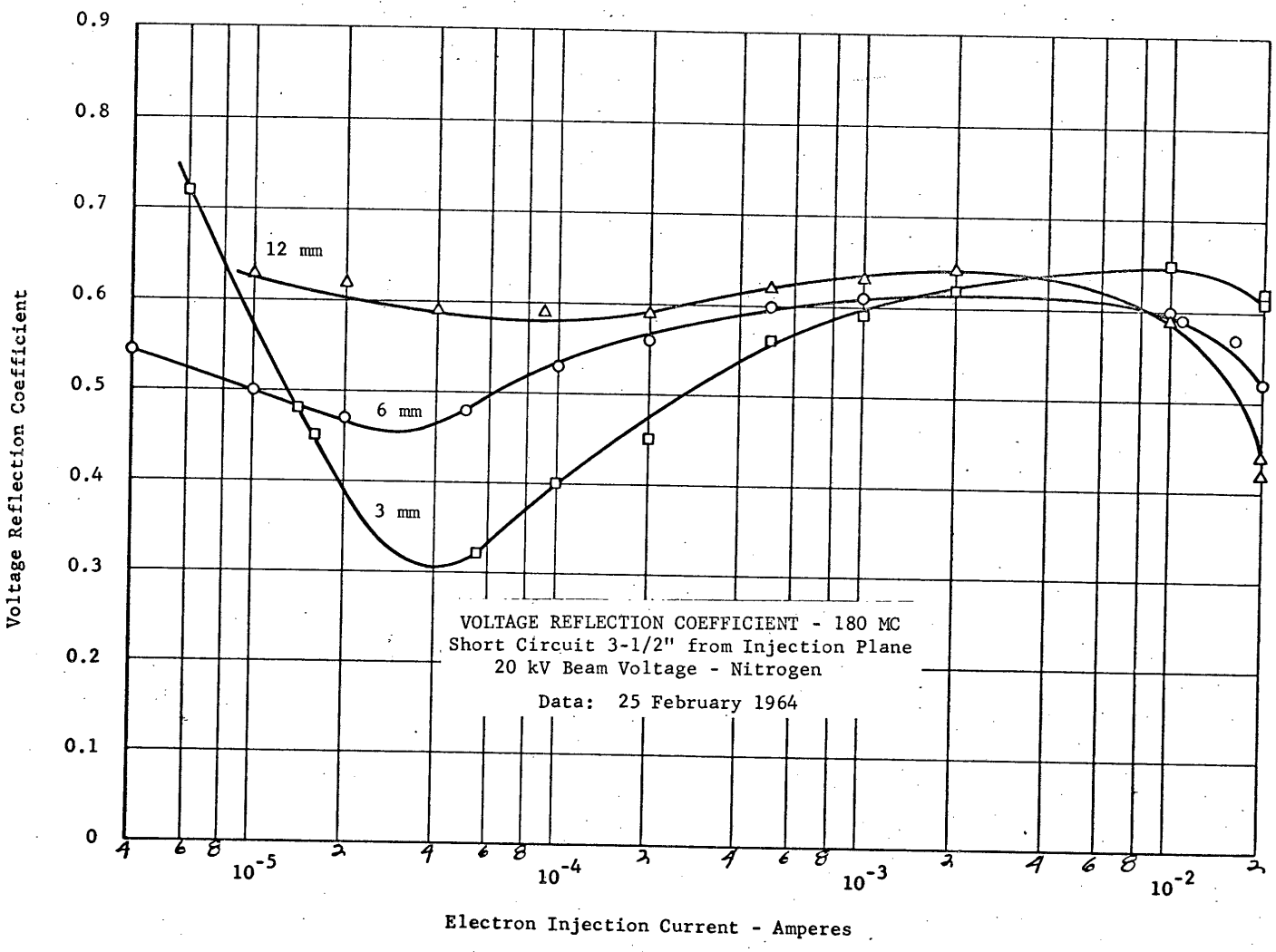

FIGURE #7

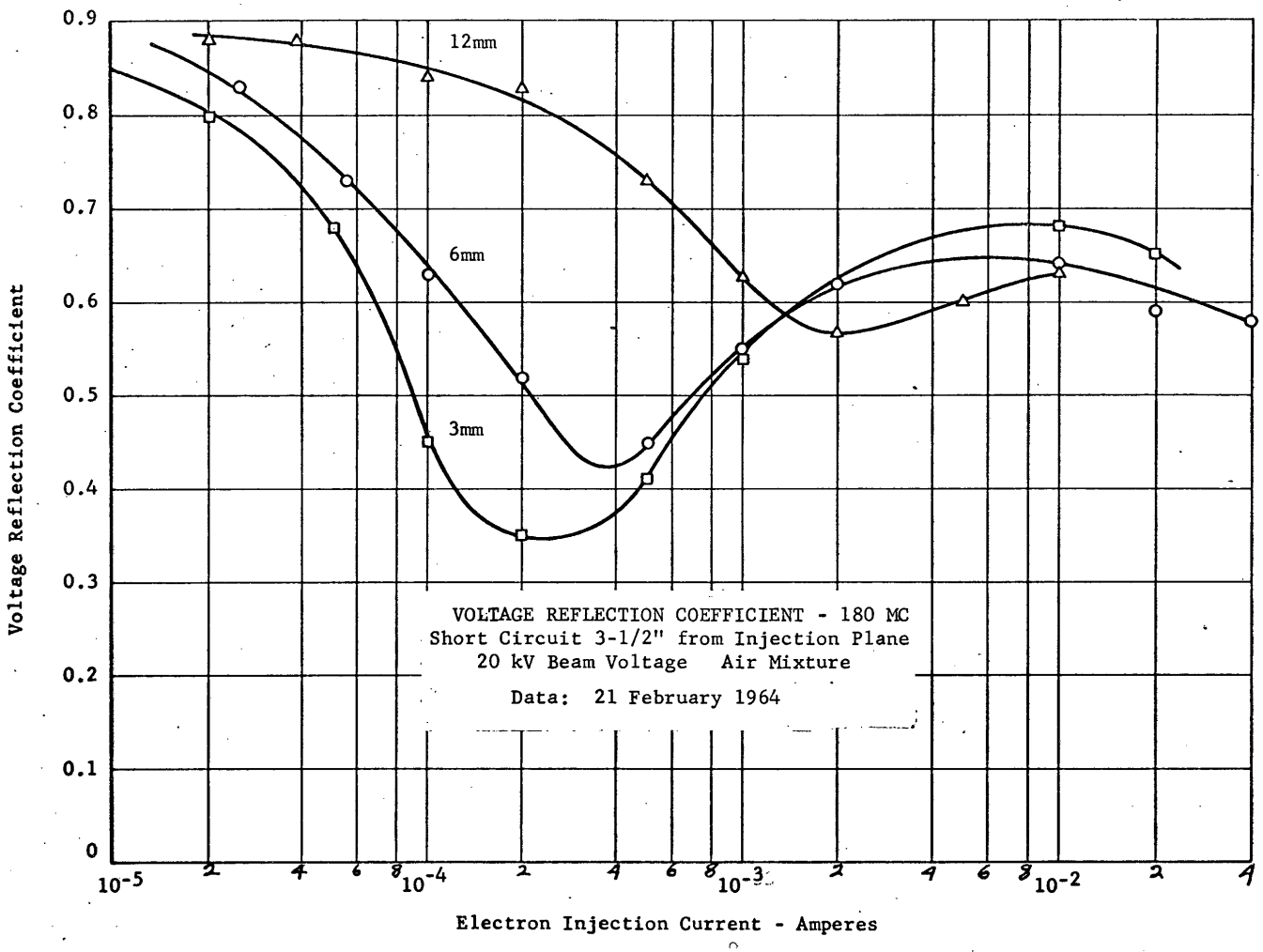

FIGURE #8

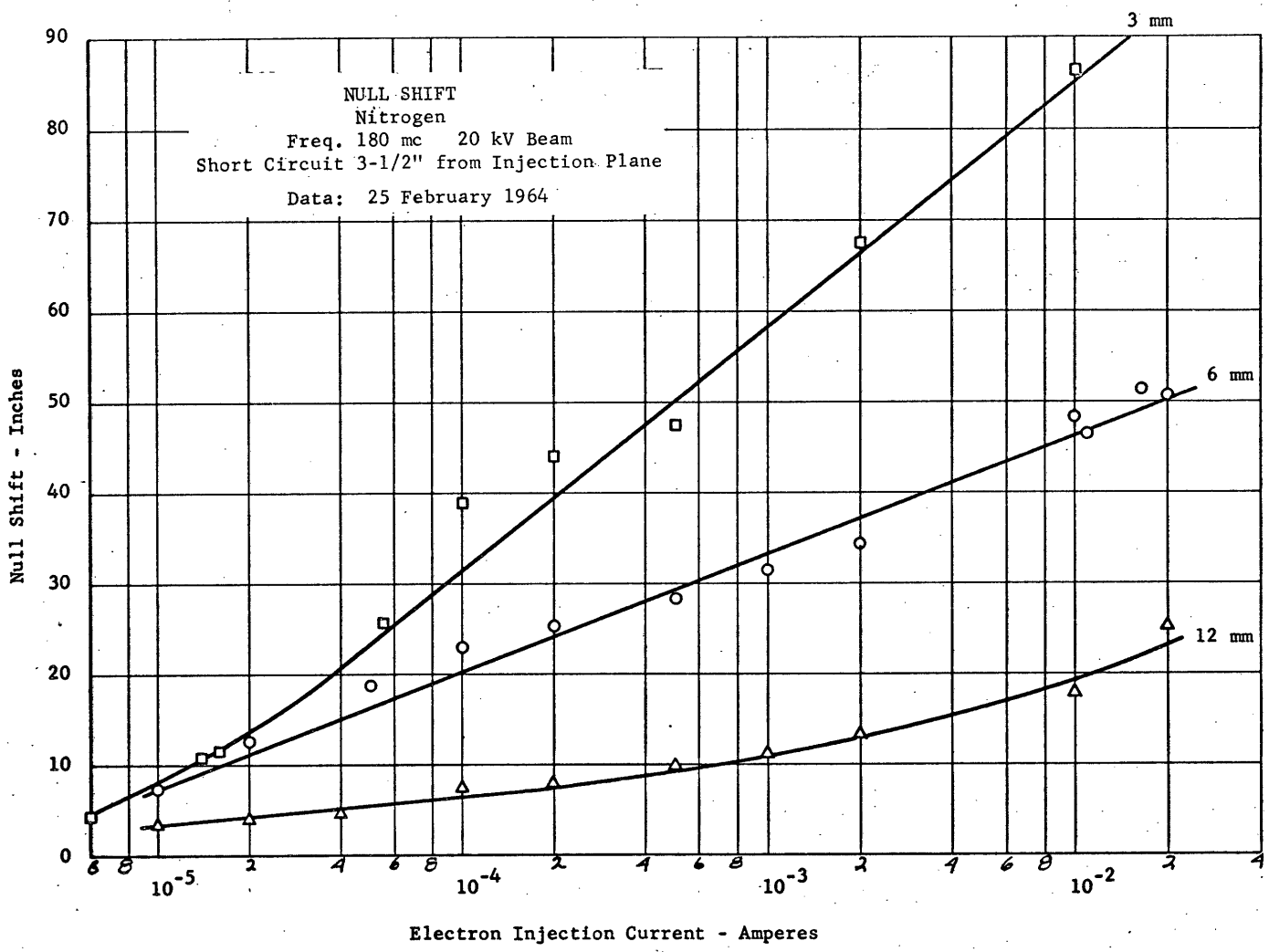

FIGURE #9

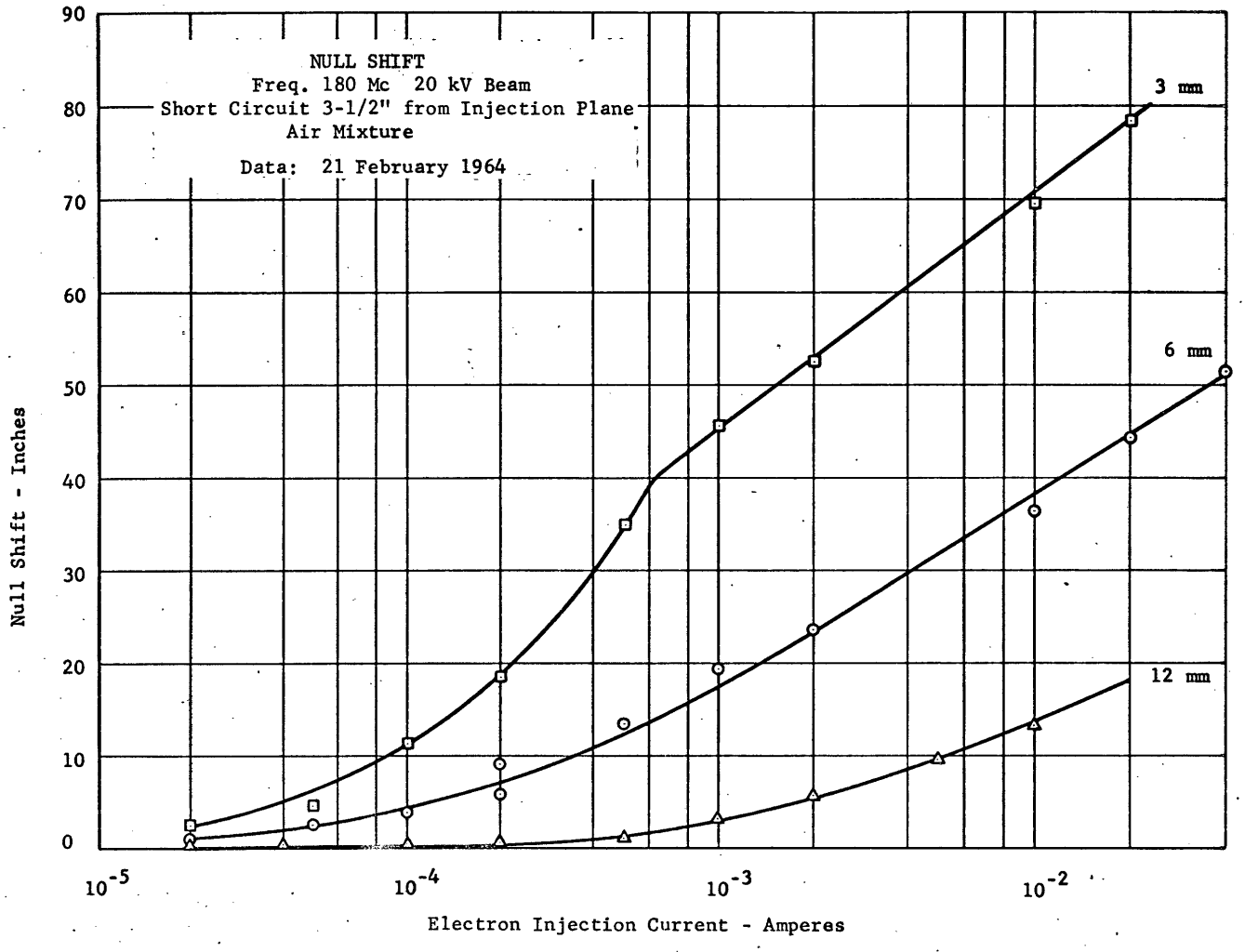

FIGURE #10

Similarly, the 3 mm null shift curve in Figure 9 for a nitrogen plasma shows a slow movement outward as the beam current is increased to about 30μ amps, and beyond this value the null shift increases more rapidly as penetration through the plasma ceases and reflection occurs off the front end of the cloud.

The reflection point roughly follows the intersection of the critical density level in Fig. 4 with the appropriate electron density profile for the beam current chosen. Thus, for example, in Fig. 9 a beam current of 2 ma yielded an effective reflection point at 66" from the injection plane, and the intersection of the critical density level with the 2 ma electron profile of Fig. 4 occurs at 64".

The value of the reflection coefficient at its minimum point is 31% in a nitrogen plasma at 3 mm gas pressure, and it occurs at a current value where probe measurements indicate that the cutoff density for the waveguide was just reached or slightly exceeded, as would be expected. However, the magnitude of the reflection at its minimum value is much greater than would be expected from the attenuation calculated for a round trip traversal of the plasma through the measured density profile for this beam current, if the calculation is made using the approximation that the density gradient is very gradual relative to a wavelength. Using this approximation, a rough graphical integration of attenuation through the varying density profile yields a value of approximately 30 to 40 db for the round trip attenuation, compared to 31% measured E wave reflection, or 10 db attenuation. The low value of measured reflection loss is attributed to mismatch type reflection from the sharp gradient of the plasma which in these experiments at 20 KV ionizing energy is short relative to a wavelength. This effect will be seen in free space plasmas as well as in the waveguide experiment, although it is probably exaggerated somewhat in the waveguide, where the propagation wavelength is greater than in an equivalent free space situation. The experimental results indicate that the theory developed for a gradually changing density cannot be used where gradients sharp relative to a wavelength exist.

The behavior of the RF wave in the air plasma is similar to that in the nitrogen plasma as is seen by reference to the air profile curve of Fig. 5 and the reflection coefficient and null shift curves of Fig. 8 and 10 for 3 mm air plasmas. For example, the minimum reflection point occurs at a beam current of 200μA in air from Fig. 8, compared to 40μA for nitrogen, and this is consistent with the higher current values required to produce a given electron density in air than in nitrogen as seen in the profile data of Figure 5.

As the pressure is increased to 6 mm and then to 12 mm, the length of the plasma cloud decreases proportionately,and presumably the sharpness of the density gradient at the outer edge of the cloud also increases proportionately. This would account for the increase of the reflection coefficient observed at the higher pressures as shown in Figures 7 and 8.

We expect a much more gradual gradient, however, in the long plasmas to be obtained at 20 mm pressure with the 150 KV gun, and correspondingly much less reflection due to sharp gradient mismatch at the outer edge of the cloud.

The beam current required to produce minimum reflection does not change much in the nitrogen plasma, indicating that the recombination loss factor is not very sensitive to pressure, at least up to 6 mm pressure. Similarly, the null point shifts shown in Figure 9 decrease in size about two to one for each reduction of two to one in pressure, consistent with the reduced plasma lengths.

The oxygen attachment loss effect in the air mixture is clearly evident in the voltage reflection coefficient behavior at different gas pressures as seen in Fig. 8. In the air plasma the current required to produce cutoff density, and hence minimum reflection coefficient, increases rapidly as gas pressure is increased, particularly above 6 mm, due to the increasing importance of the oxygen attachment loss. Similarly, the null point shifts decrease more rapidly in the air plasma than in the nitrogen plasma as the gas pressure is increased.

C. RF Attenuation Experiments

As will be discussed in a later section, the propagation characteristics of the ionized region can be shown to be comparable in free space and in a constraining waveguide. The relationship can be put into quantitative form by solution of the wave equations for the two cases. Expressions for the attenuation in the case of propagation through media with moderate conductivity, but where displacement current is still greater than conduction current are given in most textbooks on electromagnetic theory[1,2,3] and are applicable to the plasmas considered here. The attenuation for propagating waves is given by

In free space: $$\alpha = \frac{\sigma \eta}{2}$$

In waveguide: $$\alpha = \frac{\sigma \eta}{2\sqrt{1-(\frac{\lambda}{\lambda_c})^2}}$$

where σ is the conductivity of the medium

η is the wave impedance in the medium = $\frac{377}{\sqrt{\varepsilon_r}}$

λ is the free space wavelength = λ_0

λ_c is the cutoff wavelength in the waveguide = 2a

a is the waveguide width

ε_r is the dielectric constant of the medium relative to that of vacuum.

Since the guide wavelength is equal to the wavelength in the unbounded medium divided by the radical, the waveguide attenuation is equal to the attenuation in free space

times the ratio of guide wavelength to free space wavelength. This applies to densities below cutoff density, where normal propagation is possible.

The effect of the plasma, is to decrease the relative dielectric constant and to increase the conductivity. This results in bringing the waveguide to cutoff at electron densities below those of the plasma cutoff density in free space. Both in waveguide and in free space the conductivity of the plasma will reduce the reflection coefficient of the nonpropagating medium, and modify the leakage characteristic through the cutoff transmission path.

Figures 11 and 12 show the measured transmission loss obtained on a one-way transmission through the test section. In these measurements, the receiving probe was a small loop, inserted through the narrow wall of the waveguide and located 14 inches from the r-f short circuit. The shorting bars were located 3-1/2 inches from the electron beam injection plane.

The attenuation values for nitrogen were lower than expected at 3 and 6 mm pressures. At low beam injection currents the 3mm attenuation was less than 1/10 as great in nitrogen as in air, which is not consistent with the results obtained in reflection measurements, nor with the theoretical behavior based on measured electron densities. At 6 mm the attenuation in nitrogen was greater than in air up to 0.6 ma of injection current, and above that was lower. At 12 mm pressure the attentuation in nitrogen was greater, but the curves reach plateaus and then do not rise further

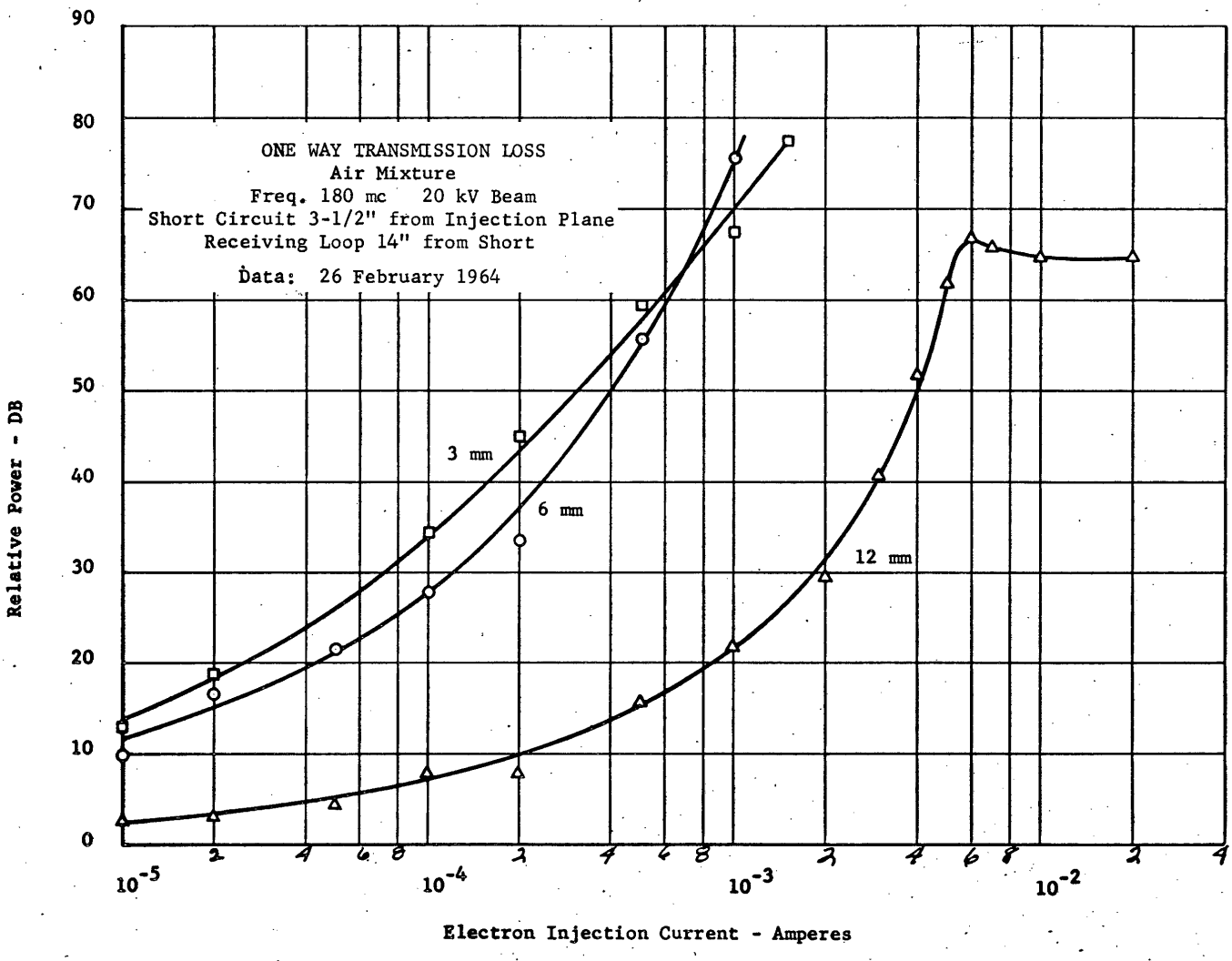

FIGURE #11

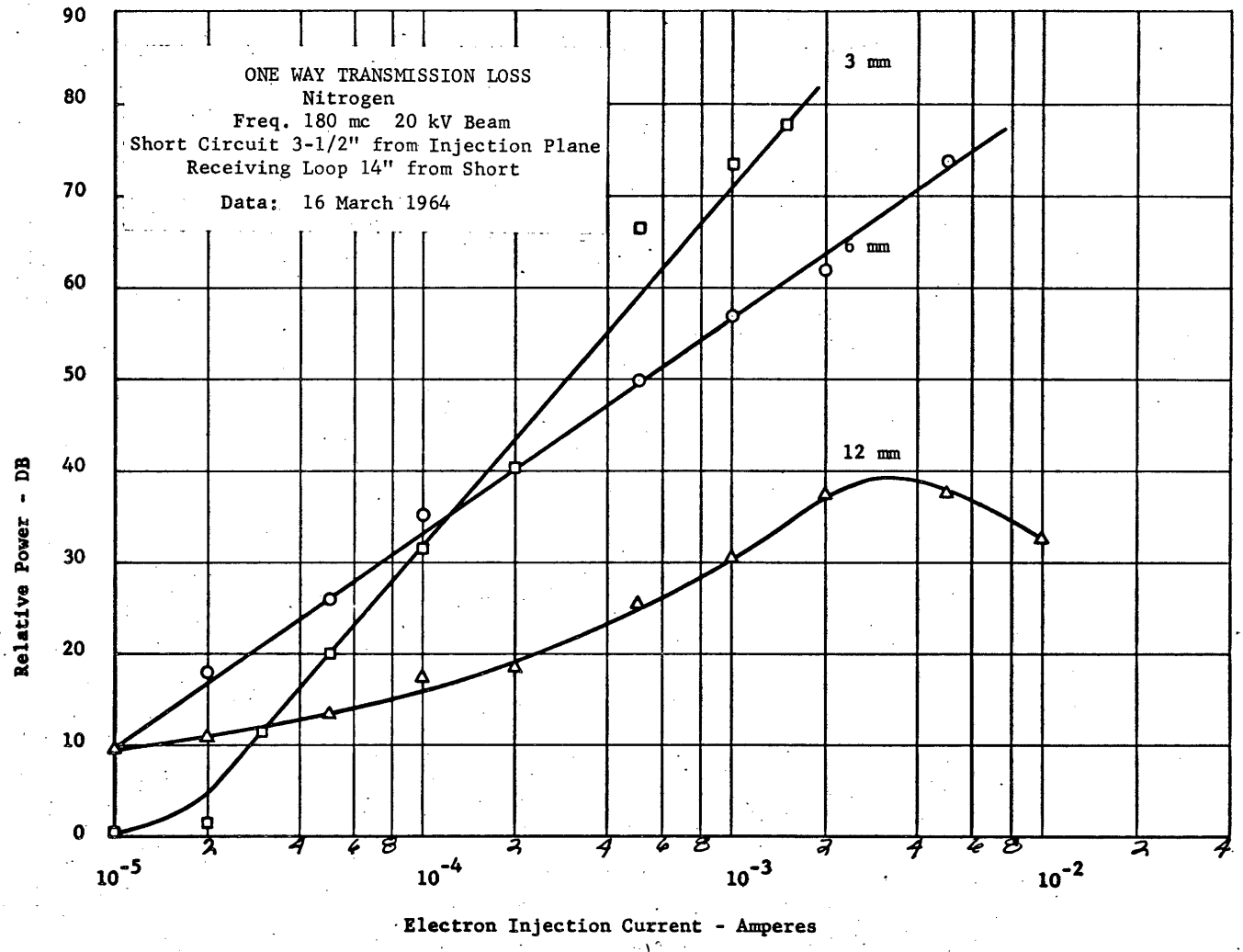

FIGURE #12

as the injection current is increased. The plateau for air is about 35 db higher than that for nitrogen. One possible explanation which has been advanced for this behavior is that the plateau represents a limit imposed by leakage in the region near the walls of the waveguide, where the electron density is appreciably lower than on axis. This effect is enhanced at the higher pressures where with only 20 KV injection energy the short range of primary electrons provides inadequate filling of the waveguide. The plasma medium is then quite nonuniform over a cross section of the waveguide with a less dense plasma surrounding the high density cores along each gun axis. Thus quite possibly the leveling off of the attenuation curves with increasing beam current was due to leakage around the cloud at the high pressures.

The experiment was designed for 3mm pressure where good filling is obtained, and we should not try to push the interpretation of the RF attenuation and reflection data too far at the higher pressures.

The primary value of the high pressure data is in the values obtained for growth and decay times, which are not particularly dependent on uniformity of filling.

Using the measured values of electron density at 3 mm pressure, it is possible to compute the transmission loss to be expected in the transmission measurements. The relationships required for this computation are

$$\epsilon = 1 - \frac{1}{\frac{\nu^2}{\omega^2} + \frac{\omega^2}{\omega^2}}$$

$$\sigma = \frac{\varepsilon \nu}{\frac{\nu^2}{\omega_p^2} + \frac{\omega^2}{\omega_p^2}}$$

where ε is the relative dielectric constant

σ is the conductivity

ν is the collision frequency

ω_p is the plasma frequency.

The attenuation is then

$$\alpha = \frac{\sigma \eta}{2\sqrt{1 - (\frac{\lambda}{\lambda_c})^2}} \quad \text{for the propagating wave} \qquad (1)$$

$$\alpha = \frac{2\pi}{\lambda_c}\sqrt{1 - (\frac{\lambda}{\lambda_c})^2} \quad \text{for the cutoff wave in the waveguide} \qquad (2)$$

$$\alpha = \frac{2\pi}{\lambda}\sqrt{|\varepsilon|} \quad \text{for the cutoff wave both in space \& in waveguide (overdense plasma)} \qquad (3)$$

In these expressions the waveguide wall attenuation is neglected for the propagating mode, since its magnitude is much less than 0.1 db., and the plasma conduction loss is neglected for the cutoff conditions, since the reactive attenuation is much greater than the dissipative attenuation.

For the computation, the number densities at stations one foot apart were used. The plasma was then assumed to consist of discrete layers, one foot thick, each having uniform characteristics. A summation of the attenuations in the layers was then taken as the total plasma attenuation.

The attenuations computed for one way transmission loss in the underdense plasmas at very low beam currents were in very poor agreement with the measured attenuations both for air and for nitrogen, and the reason for this was not found. This may have been due to experimental difficulties or it may have been associated with the reaction of the plasma on the loop used to measure the H field near the injection plane. These discrepancies should be explored further in the 150 KV equipment.

However, fair agreement, within about ± 20% in terms of electron density, was obtained between the very large calculated and measured attenuations for the evanescent wave in the overdense plasmas. For example, for 2.0 ma beam current the agreement between calculated and measured values was as follows:

Air 2ma $\nu = 10^9$

Station	Electron Density	Attenuation	Measured Attenuation
7	7.5×10^7	0.9 db	
6	4.0×10^8	4.1	
5	1.1×10^9	7.3	
4	1.8×10^9	12.3	
3	2.8×10^9	17.2	
2	3.4×10^9	19.4	
Reflection loss		1.9	
		79.1 db	83.db

Nitrogen 2ma $\nu = 10^9$

7	1.0×10^8	1.2 db	
6	7.0×10^8	7.6	
5	2.0×10^9	13.4	
4	4.5×10^9	22.4	
3	6.0×10^9	27.2	
2	6.0×10^9	27.2	
1	4.0×10^9	21.3	
Reflection Loss		1.9	
		122.2 db.....	83. db

The discrepancy for nitrogen is rather large while reasonably good agreement is obtained with air suggesting that the measured 2 ma electron density profile for nitrogen at 3 mm is too high. It also appears too high from the point of view of its relationship to the nitrogen profiles at 20 ma and at .2 ma.

It should be noted that strictly speaking equation (3) for the attenuation of the evanescent wave applies only to free space conditions; we are assuming without mathematical confirmation that it also applies without correction to the waveguide. In any case, these calculations and measurements for attenuation in the overdense plasmas are only of secondary interest, since reflection off the front edge of such a plasma is the dominant mechanism of interest as far as net reflection effect is concerned.

The slow gradient approximation has but little effect here since the reflection loss was small compared to the very large transmission loss and was known.

---

1. S. Ramo and J. Whinnery, "Fields and Waves in Modern Radio", Chapter 9, John Wiley & Sons, 1944.

2. E. G. Linder, "Attenuation of Electromagnetic Fields in Pipes Smaller Than the Critical Size," Roc. IRE, p. 554, Dec. 1942.

3. V. L. Ginzberg, "Propagation of Electromagnetic Waves in Plasma," pp. 640, 641, Gordon and Breach, 1961.

D. PLASMA GROWTH & DECAY RATE CHARACTERISTICS

A series of measurements were made of the temporal growth and decay characteristics of both nitrogen and air plasmas at various pressures. These were undertaken with a two-fold purpose - first, to determine actual growth and decay rates at 20 mm pressure for direct application to the project, and second, to obtain basic data from which recombination, attachment and diffusion constants might be obtained.

The tools available for this task were only qualitative as far as determination of instantaneous values of electron density is concerned. Although the pulsed deflection of the entering beam allowed a rapid switching on and off of the exciting beam, we had no direct method of measuring electron densities on a quantitative basis. We used the Langmuir probes as one source of data for these qualitative measurements and the RF reflection output from the directional coupler as another. Neither of these gives direct electron density data during transient conditions, but both give a qualitative picture of what happens.

The probes were used with a constant applied voltage of +3 volts relative to the chamber, and the transient rise of current in the probe was indicated on an oscilloscope by the transient voltage drop across a resistor in series with the probe. It is certainly true that just preceding the excitation of the plasma there was no measureable probe current and that at some later time the probe current reached a steady value, so that the approximate time constant of electron growth was obtained. However, there is no assurance that the instantaneous probe current is directly proportional to the electron density at all values of time during the transient growth and decay.

Similarly, the instantaneous change in RF reflection coefficient is certainly not proportional to the instantaneous electron density, especially since the reflection coefficient first decreases to a minimum and then increases slowly to a fairly constant value as electron density is progressively increased.

Nevertheless, in spite of these shortcomings, the inspection of the growth and decay characteristics of both probe current curves and RF reflection coefficient curves yields some valuable data as to approximate actual growth and decay rates and as to trends in these rates for various beam currents and gas pressures.

If the dominant loss mechanisms in the plasma are recombination, attachment, and diffusion, then equations can be derived predicting both the growth and decay characteristics for nitrogen and for air. The equations show that if simple recombination is the only important mechanism, the growth characteristic is a hyperbolic tangent function of time, and the decay characteristic is hyperbolic with time- i.e., shows a linear plot of 1/n vs time in the latter case. If attachment and diffusion are also important, as in air plasma, both the growth and decay characteristics follow more complex functions of the plasma constants and of time.

In general, although the detailed growth and decay characteristics follow somewhat different laws, it can be shown theoretically that the times required to decay to some arbitrary value such as 1/e of the initial value or to grow to within 1/e of the final value differ only by a constant for a particular gas at a particular current and pressure. For example, assuming simple recombination only in nitrogen, the decay time on the conventional 1/e basis is 2.3 times as great as the growth time. If the growth and decay processes were simple exponentials, their time constants would of course be equal.

The other generality deduced from the equations is that both decay and growth times expressed as conventional 1/e percentages decrease with increasing values of initial or final electron densities and hence of initial or final beam current. Furthermore these times should both also decrease rapidly as pressure is increased in the air plasma, since attachment losses increase rapidly with pressure. In nitrogen the growth and decay times should decrease more gradually with increasing pressure

because of the slower increase of recombination losses with increasing gas pressure.

So much for the expected behaviour - now as to the actual observed behaviour, the expected trends of decreasing time constants with increasing pressure are observed both for nitrogen and for air plasmas as seen in Fig. 13 and Fig. 14. As one would expect, the time constants decrease more rapidly with pressure in air than in nitrogen due to the increasing effect of oxygen attachment with pressure. Furthermore, the growth times decrease as expected with increasing values of final density (or beam current). The decrease of growth time with increasing beam current is shown more clearly in Figures 15 and 16.

Here also the data matches the expected behavior quite closely. To a first approximation the growth time constant should vary as $1/\sqrt{\alpha I}$, if attachment and diffusion are ignored, so that when current is plotted against time on log-log paper the slope should be - 1/2 assuming α is constant over the current range. The actual data in Figures 15 and 16 has slopes ranging from -.32 to -.62 and the smaller slopes appear in air plasma where attachment is important.

The behaviour of the decay time, however, as a function of beam current is surprising. According to the simple theory outlined above the decay time expressed as the time required to reach some arbitrary percentage of the final value should decrease with increasing beam current, whereas in fact it shows almost no variation with beam current, so that at 16 ma beam current the decay time is more than an order of magnitude greater than the growth time.

This is a real effect at least under our experimental conditions since these measurements were repeated many times with small variations in the experimental techniques but the trends were always consistent and they showed up both in the probe measurements and in the RF reflection measurements. Apparently some other mechanism beyond recombination is operative during the afterglow in nitrogen which holds the time constant up as the initial density is increased.

Figure 17 demonstrates the need for interpretation of the growth and decay characteristics as obtained directly by the RF and probe methods. The upper set of curves shows normalized growth and decay responses by both methods. A measure of the time to grow to within 1/e of the final value or decay to 1/e of the initial value directly from the curves of probe and RF responses would yield values differing by two or three to one. The RF responses measured across a crystal inserted in the reflected wave output of a directional coupler respond to RF reflected power. Thus the RF growth and decay characteristics are more properly shown in the bottom set of curves of Figure 17 as per cent of power reflected through a plasma. It is difficult to relate the transient behavior of the RF reflected power with the growth and decay of electron density in any quantitative way other than to say that the conventional measure of 1/e time constants will be too short in growth and too long in decay.

For example, if we consider the transient curves shown for an air plasma at 12 mm pressure with 10 ma beam current as in Fig. 17, and also note from Figure 8 that the steady state reflection coefficient reaches a minimum value at only 2 ma beam current, we realize that in the transient growth condition the electron density will reach the value required to produce maximum effect on reflection long before the final value is reached, since the reflection coefficient does not change appreciably for the higher densities reached at 10 ma. Thus the RF reflection growth response will be speeded up several fold in time compared to the growth of electron density. On the other hand, in the decay regime, the electron density will fall several fold before its effect is seen in a change in the RF reflected wave, so that the decay time of the reflected wave is several fold longer than the decay time of the electron density. Therefore, the RF and probe transient response curves should differ in the way actually observed in Fig. 17. No doubt the probe curves are closer to the true electron density characteristic for this reason.

It is true, however, that 1/e time constants measured by the RF method will be more closely related to density time constants at high pressures of 20 mm or at low beam currents, because under these conditions the relationship of reflected power to electron density is more nearly linear. Indeed, where those conditions were met, the time constants measured by RF and probe methods were in close agreement.

The transient curve probe measurements referred to in the growth and decay experiments were taken at 36" from the injection plane for pressures of 3 and 6 mm, and at 12" from the injection plane for 12 and 20 mm pressures. The RF reflection effects are of course dependent on values of electron density throughout the plasma, but the shape of the transient curves measured at the sample points with the probes are probably generally representative of the shape of the transient growth or decay of density throughout the plasma.

PLASMA GROWTH AND DECAY IN NITROGEN VS PRESSURE AT DIFFERENT INJECTION CURRENTS

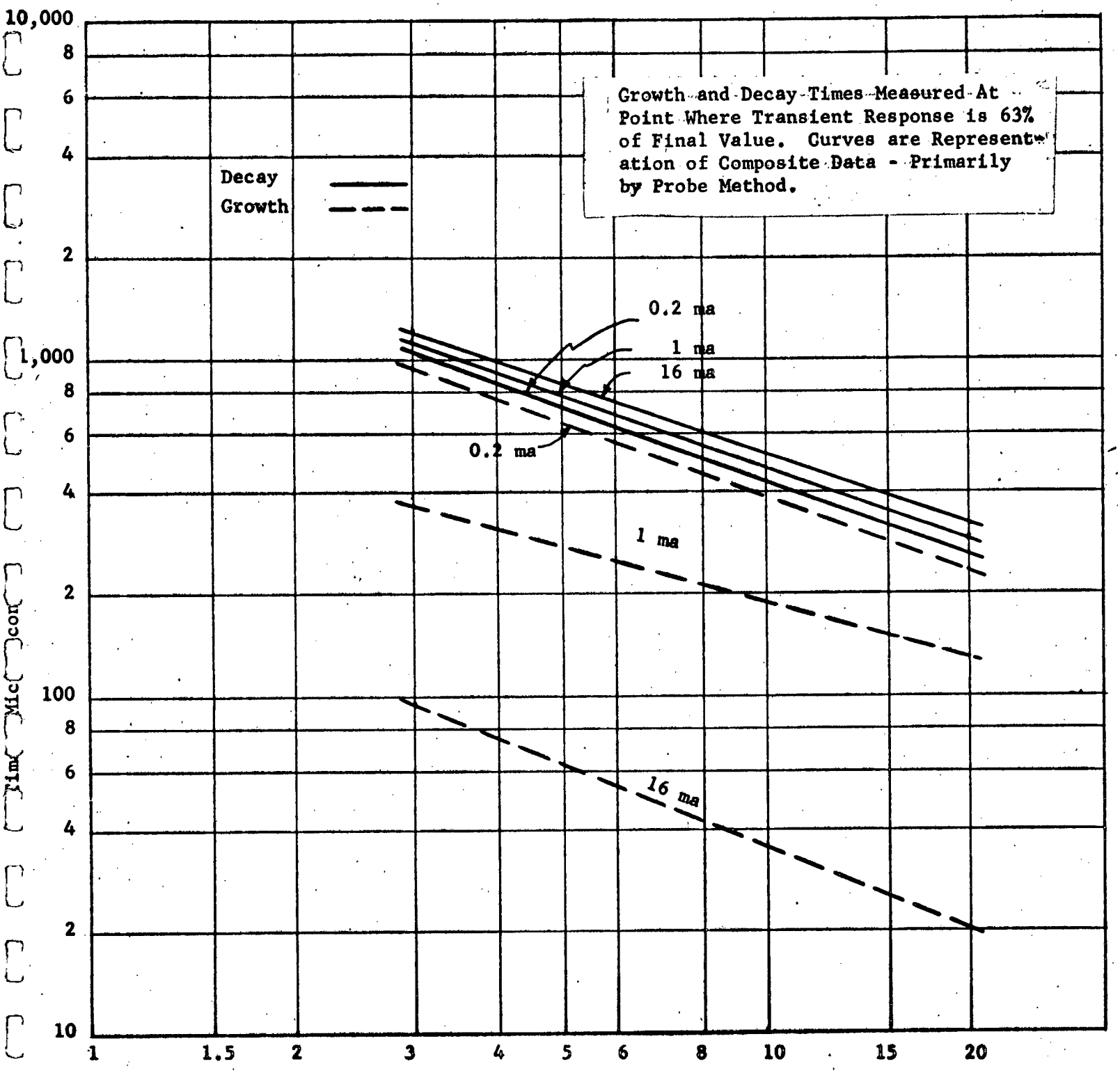

FIGURE #13

PLASMA GROWTH AND DECAY IN AIR
VS
PRESSURE AT DIFFERENT INJECTION CURRENTS

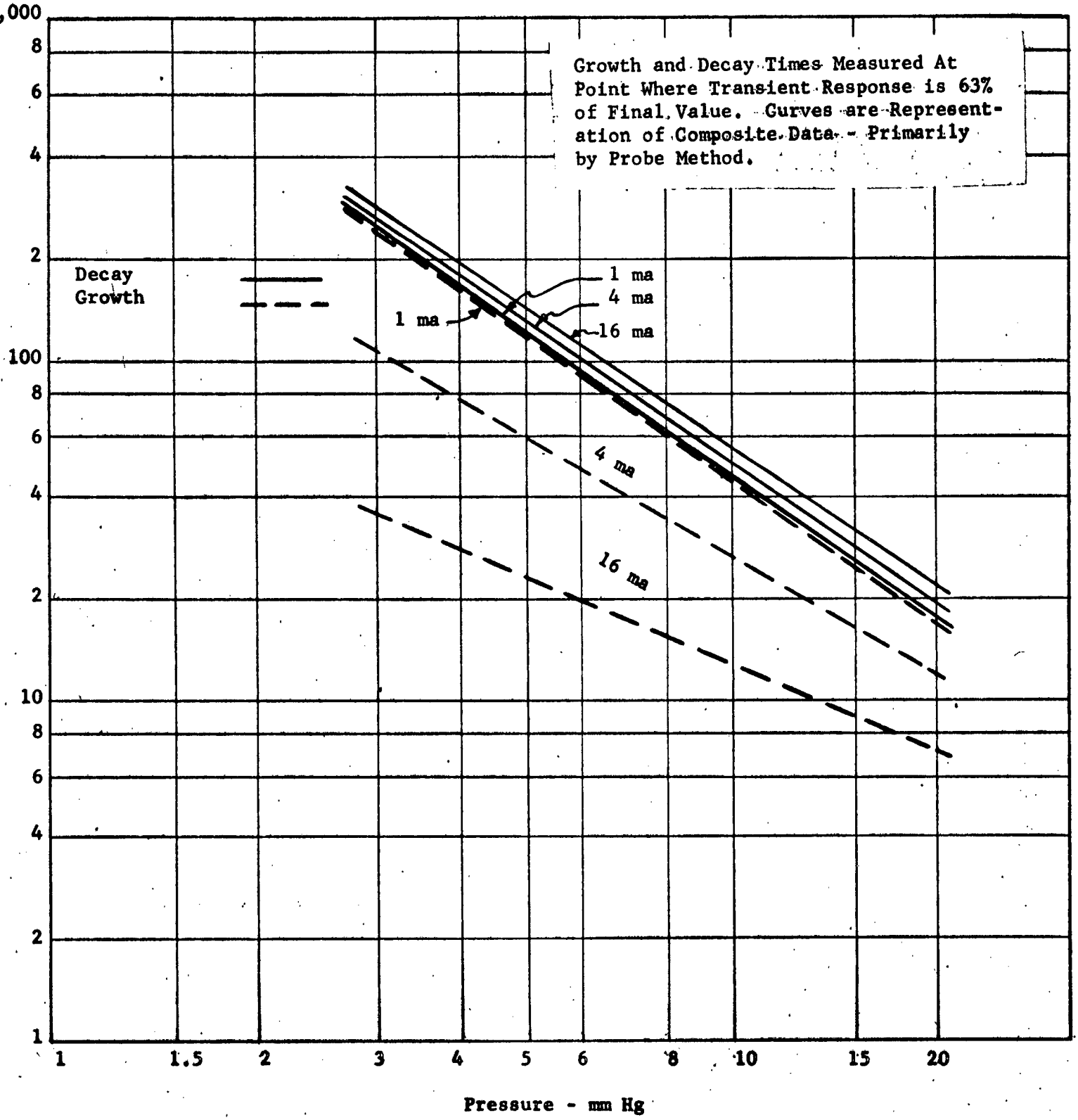

FIGURE #14

PLASMA GROWTH AND DECAY IN NITROGEN
VS
INJECTION CURRENT AT DIFFERENT PRESSURES

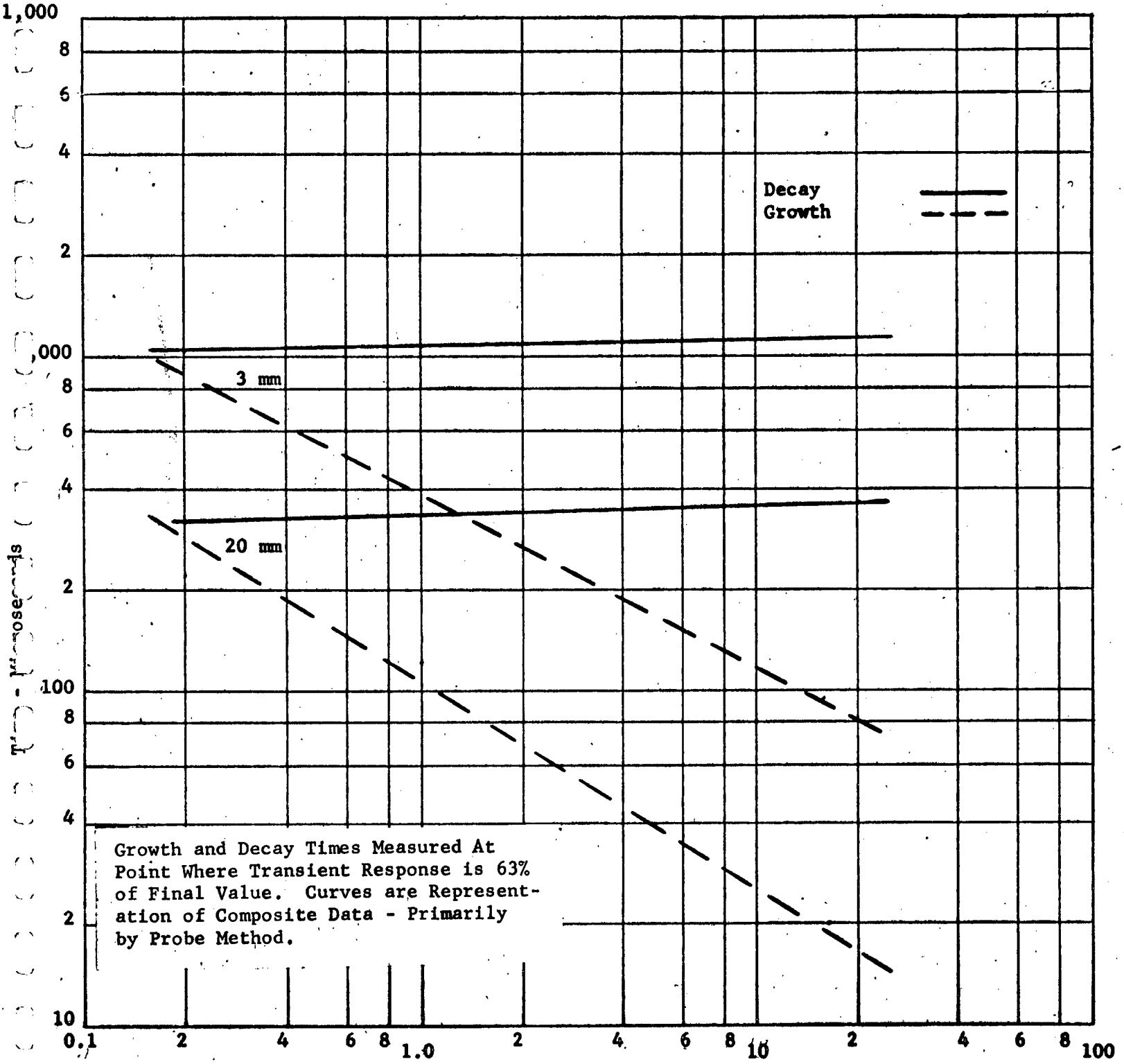

FIGURE #15

PLASMA GROWTH AND DECAY IN AIR
VS
INJECTION CURRENT AT DIFFERENT PRESSURES

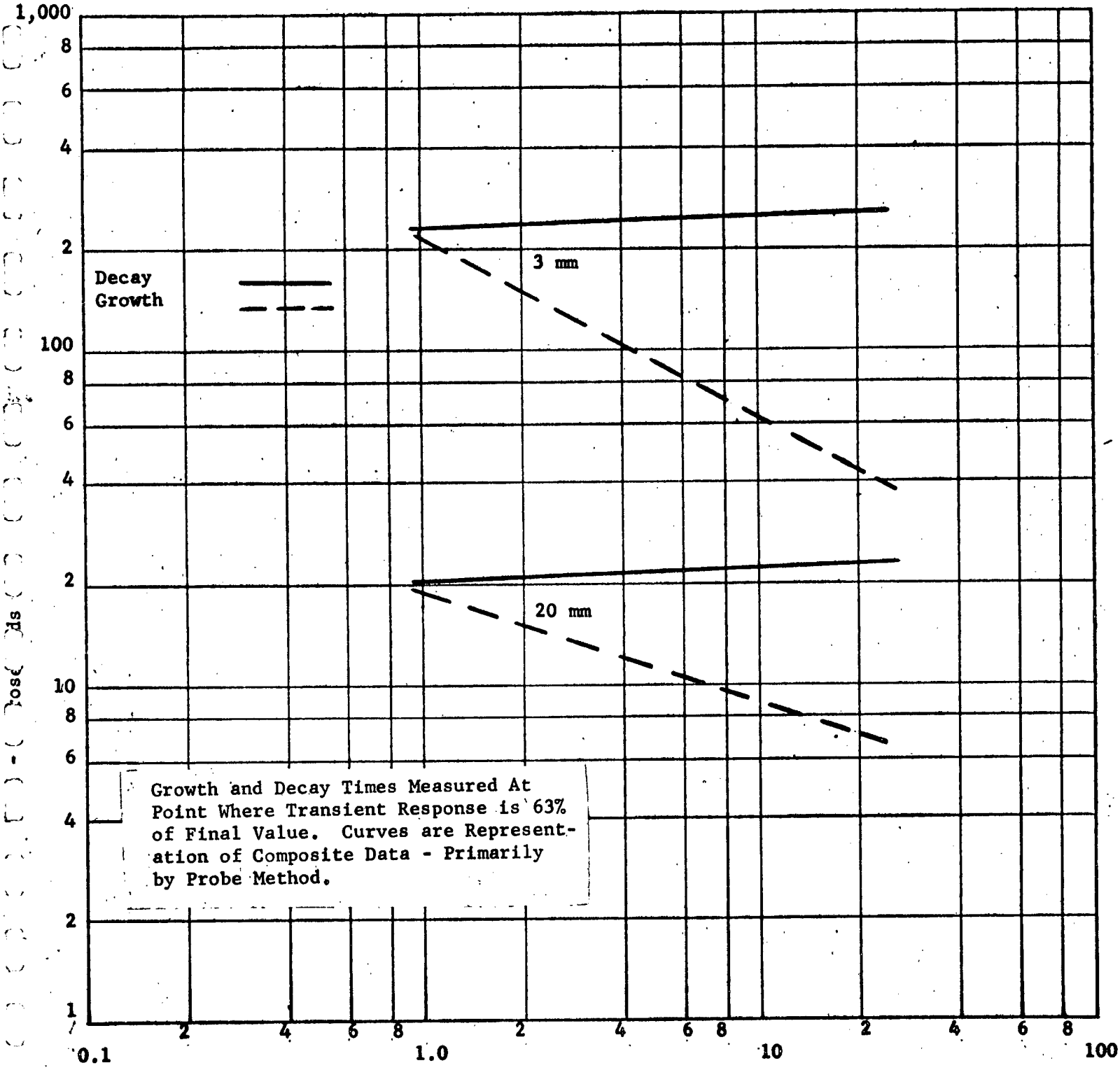

FIGURE #16

GROWTH AND DECAY CHARACTERISTICS-PROBE AND RF METHODS

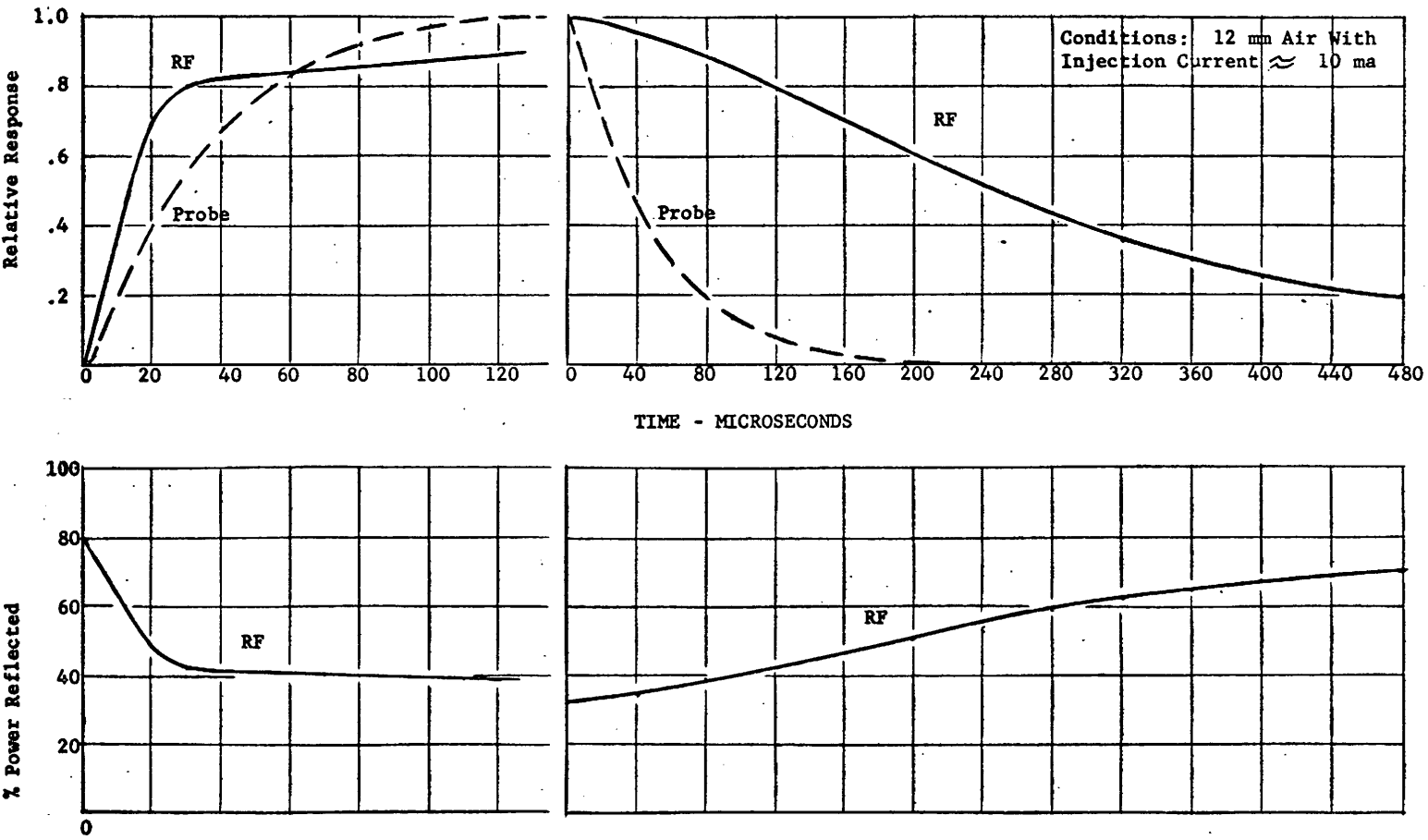

FIGURE #17

E. SOME RESULTS AT 20 MM PRESSURE

At 20 mm gas pressure the 20 KV beam energy is sufficient to produce only a small plasma cloud of generally hemispherical shape except for the diverging incident primary beam jet. The size of the two plasma clouds was estimated visually to be about 10" - 12" diameter.

Thus as far as the incident electromagnetic wave is concerned, reflection and transmission phenomena are governed by thin slab theory, since the free space wavelength is seven times as thick as the plasma clouds, and the hemispherical clouds do not quite touch the walls of the waveguide.

Nevertheless, it is of interest to study the reflection coefficient and the apparent reflection point for this condition. The results are shown in Fig. 18 for varying beam current. It is noted that the reflection coefficient starts decreasing even at very low beam currents and then decreases steadily as beam current is increased up to about 15 ma. For currents above 15 ma (300 watts injection power) the reflection coefficient levels off.

The apparent reflection point shows no measurable change up to currents of about 5 ma and then rapidly moves out to a saturation value of 12", indicating again reflection from the front edge of the cloud. The curves break at about 12 ma, and it is presumed that a waveguide cutoff density of 2.8×10^8 per cm^3 is reached in this region of current.

This behaviour illustrates qualitatively the presence of the much higher attachment losses in air at 20 mm than at lower pressures where cutoff density is reached at much lower beam currents.

More meaningful, however, are the growth and decay time measurements at 20 mm, since these should not be affected by the size of the plasma. Both the probe and the RF measurements indicate growth times in the order of 10 microseconds for the higher beam currents in an air plasma at 20 mm pressure, and a decay time in the order of

20 microseconds for all currents.

The behaviour of the growth in the first microsecond was examined, and a persistent delay of about 300 nanoseconds was observed in the start of the RF response. This did not show up either in the first microsecond of probe current response nor in the first microsecond of light response measurements made with a photomultiplier. It may yet be in the RF instrumentation, although every effort was made to remove such a limitation.

REFLECTION COEFFICIENT & POSITION OF STANDING WAVE NULL VS EXCITING BEAM CURRENT

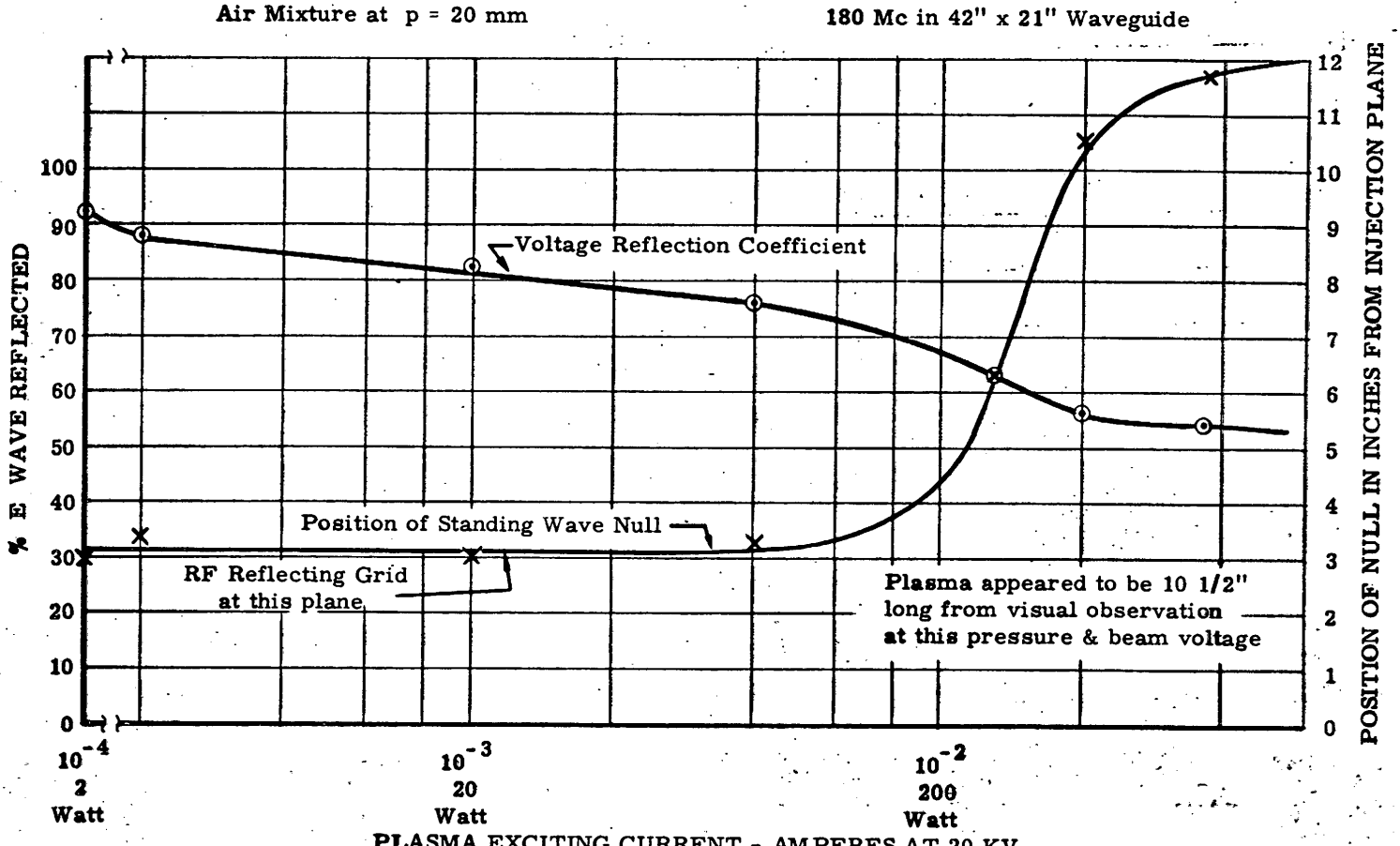

FIGURE #18

Figure 10

F. OTHER EFFECTS

As mentioned in previous reports no effect on either a nitrogren or an air plasma was observed by irradiation with an ultraviolet source having an intensity of four suns in the UV region. This test was repeated a number of times at various pressures and no detectable effect was observed.

A fast acting differential pressure sensor introduced into the main chamber showed that under steady state excitation there was an increase of pressure of about 6 - 10% when high beam currents were introduced into the chamber, and a similar decrease when the beam was removed. The time constant of this effect was about 2 seconds and it is attributed to a rise in gas temperature at the high beam powers.

The fast time scale growth and decay times described in this report, however, were all made under "cold gas" conditions. For these measurements the cold gas was excited by a beam for less than 100 microseconds and then excitation was removed. Presumably the gas temperature did not change appreciably during this short excitation.

IV. DERIVATION OF PLASMA CONSTANTS

A beginning was made on the derivation of electron loss mechanism coefficients from the observed data on growth and decay times and on electron production efficiency. If we assume that losses consist of two types; those varying as n, and those varying as n^2, then we may write an equation for the net rate of change of electron density at some point in the plasma as follows:

$$\frac{dn}{dt} = \Gamma I - \beta n - \alpha n^2$$

where n is the electron density in electrons per cm^3, ΓI is the formation rate in electrons per cm^3, α is the recombination coefficient in cm^3/sec, β is a term including diffusion loss in nitrogen, and diffusion plus attachment in air.

In the steady state situation, $\frac{dn}{dt} = 0$ and $\Gamma I = \beta n + \alpha n^2$.

We now take steady state density points at a two foot distance from the injectors from the profile data shown in Figures 4 and 5 for the nitrogen plasma and the air plasma and plot them against beam current as shown in Figure 19. We then can plot a curve through the nitrogen points and another through the air points, as also shown on Figure 19. A value of Γ, the production efficiency in number of secondary electrons per primary electron per cm^3, can be estimated from the observed size of the primary beam at 2 ft from the apertures and from calculated values of the formation rate for this fraction of the total range of 20 KV initial energy electrons. This yields a value

$$\Gamma = 3.4 \times 10^{15} \text{ cm}^{-3}$$

Knowing Γ and assuming that the diffusion losses are equal in the nitrogen and air plasmas we can then derive approximate values of δ, the diffusion coefficient, β, the attachment coefficient, and α, the recombination coefficient to give a best fit to the observed curves of Figure 19.

A fair fit is obtained for the following values of the coefficients:

$\alpha = 3.2 \times 10^{-7}$ cm^3 per sec for recombination at 3 mm pressure

$\delta = 1.9 \times 10^{2}$ sec^{-1} for diffusion "

$\beta = 7.8 \times 10^{2}$ sec^{-1} for attachment "

$B = \beta + \delta = 9.7 \times 10^{2}$ for diffusion plus attachment "

The value of α is in fair agreement with values reported in the literature, and the value of β is in fair agreement with the data of Bionde and Chanin for an equivalent range of electron densities. Values of β reported by others are generally much higher, but they may apply to different plasma conditions.

Values of α, β, and δ may also be obtained from the growth time data, but time did not permit completion of that analysis.

RELATIONSHIP OF ELECTRON DENSITY WITH INJECTION CURRENT

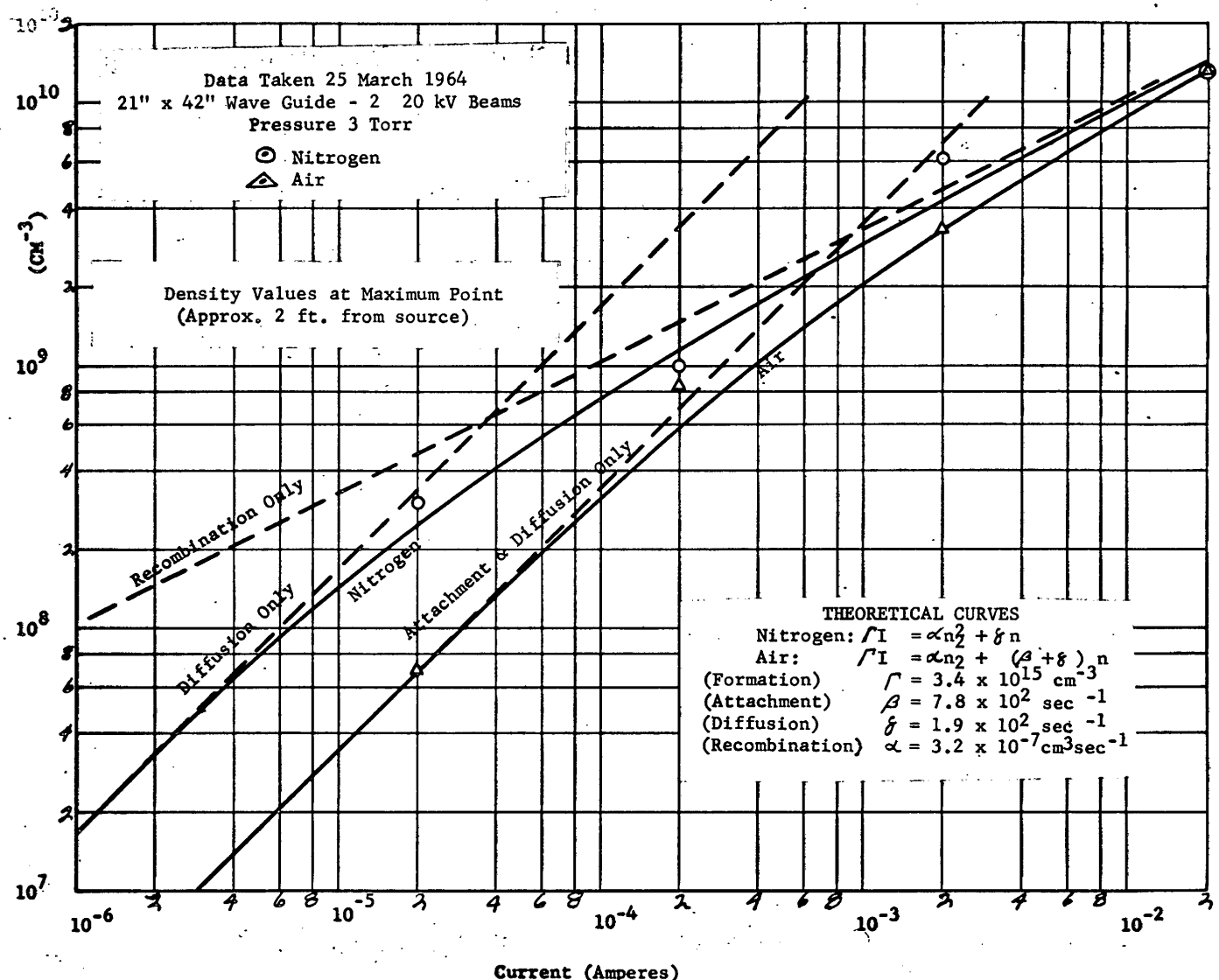

V. Relation of Waveguide to Free-Space Conditions

Some understanding of the relationship between waves in an unbounded free-space plasma and waves in a plasma bounded by metallic waveguide walls is necessary for a proper interpretation of the results obtained from the waveguide measurements. This discussion of that relationship will be limited to plasmas which vary in one direction only and are uniform in planes perpendicular to that direction, such planes being infinite for free space and the rectangular cross section for waveguide.

There are two limiting cases for the variation in the plasma density: (1) it may change rapidly from zero to some large value within much less than one wavelength, in which case it behaves like an abrupt discontinuity in the medium and produces a reflection from the surface, and (2) it may vary very gradually over many wavelengths from zero to a large value, in which case the wave enters it and is gradually refracted and attenuated. The intermediate case of moderate plasma variation within a wavelength is more difficult to analyze and depict, because both reflection and transmission with refraction occur at all points along the path of any ray and produce a resultant emerging wave that can vary considerably with the plasma parameters.

For purposes of initial discussion, consider the case of a gradually increasing plasma density as shown in Figure 20. If a plane wave is incident so that its direction of propagation makes an angle θ_1 with the normal to the plasma as shown, the individual rays will be bent further and further from the normal until they become perpendicular at that plasma density for which the

refractive index, n , becomes equal to sin θ_1.[1] The rays continue to bend away from their original direction and leave the plasma at an angle of $(180^\circ - \theta_1)$ from the normal. For waves incident at smaller angles to the normal, the individual rays penetrate further into the plasma, as shown for rays at angles θ_2 and θ_3 with the normal.

The greatest penetration occurs for normal incidence, in which case the rays are along the normal and return on themselves from a depth at which the refractive index is zero. For a lossless plasma, the refractive index is zero at a plasma density given by $N = (f/9000)^2$, where N is the density in electrons per cubic centimeter and f is the frequency in cycles per second. For a plasma with loss, the penetration is slightly greater to a plasma density given by:

$$N = \frac{f^2}{9000^2} \left[1 + \left(\frac{\nu}{\omega} \right)^2 \right]$$

where ν is the collision frequency and $\omega = 2\pi f$. The wave is attenuated in the latter case as well as being refracted.

Consider next the way in which the wavefront behaves during refraction for a wave incident at angle θ_i to the normal, as shown in Figure 21. All individual rays must behave the same and the wavefront must remain normal to the rays, thus cusps are formed in the wavefronts as shown. For clarity, the inward traveling portions of the wavefronts are shown solid and the fully refracted or outward traveling portions are shown dashed. As the wave penetrates deeper into the plasma, the dielectric constant decreases and the wavelength increases as shown; thus the wavefront folds over on itself and returns out of the plasma, suffering attenuation if the plasma has loss.

1. E. C. Jordan, "Electromagnetic Waves and Radiating Systems," p.664, Prentice-Hall; 1950

Consider now the detail section of a wave refracted by a region of increasing plasma density shown in Figure 22. This is merely an expanded portion of Figure 21 with more wavefronts and no complete rays. Note that planes of symmetry exist as shown by the dashed lines. If a second wave at the same frequency were incident on this same plasma at an angle $-\theta_i$, it would have identical wavefronts traveling in the opposite direction and an interference pattern would be produced. Assume the electric vector is perpendicular to the paper. If the spacing between the wavefronts shown were one-quarter wavelength and if the pair of waves were in phase along a line of symmetry midway between the two shown, the inward traveling pair of waves and the outward traveling pair of waves would each produce nulls along the planes of symmetry shown. This would be true regardless of whether the plasma were attenuating or not, because each wave in the inward traveling pair would be attenuated the same amount and thus completely cancel all along the lines of symmetry, and likewise for the outward traveling pair. The only effect of attenuation, then, is to decrease the amplitude of the outward traveling pair of waves while preserving nulls along the planes of symmetry.

It is thus permissible to insert conducting planes along the lines of symmetry and perpendicular to the plane of the figure without changing the field configuration, assuming that the waves can be launched between the metal plates initially and that the plasma distribution is not affected by them. By placing two more metal plates parallel to the plane of the figure to terminate the electric field and with a separation of less than one-half wavelength, a portion of the given free-space distribution is completely reproduced within a rectangular waveguide of standard size for the given wavelength. This is shown in Figure 23(d).

Now it is well known from waveguide theory that the TE_{10} mode in rectangular waveguide can be expressed as the sum of two TEM waves having directions of propagation making angles θ_i and $-\theta_i$ with the waveguide axis, thus the conditions described above are exactly those which produce the TE_{10} waveguide mode for both the inward pair of waves (incident TE_{10} wave) and the outward pair of waves (reflected TE_{10} wave). The wavelength along the waveguide axis is related to that in the plasma by the relation:

$$\lambda_g = \frac{\lambda_p}{\sqrt{1 - \left(\frac{\lambda_p}{2a}\right)^2}}$$

where "a" is the waveguide width. For a uniform plasma, this relationship is constant along the waveguide as shown in Figures 23(a), (b), and (c) for three different values of plasma density and their corresponding values of λ_p and θ_i. In each of these three cases, the wave travels down the guide unchanged, except for being attenuated if the plasma has loss, and is only reflected to form a standing wave when a short circuit (S.C.) is provided as shown.

For the case of increasing plasma density shown in Figure 23(d), on the other hand, no short circuit is needed since the wavelength in the plasma, λ_p, increases along the length of the waveguide from its initial value at the input until it becomes equal to twice the waveguide width, a, at which point θ_i becomes equal to 90°. The wave then returns back from that point as though it were an effective short circuit, just as the refracted wave did in the free space plasma of Figure 22. The two component TEM waves that make up the waveguide TE_{10} mode are at that point traveling in opposite directions across the waveguide ($\theta_i = 90^\circ$) and then continue back along the waveguide to form the reflected TE_{10} wave. If the plasma

has appreciable loss, then both the forward and the reflected waves will be highly attenuated and result in a lower input VSWR to the waveguide than for a low loss plasma.

A further helpful comparison can be made of the wavefronts in Figure 22 with those in Figure23(d) by considering those portions of the wavefronts outside the dashed lines in Figure 22 to be those in Figure23(d) as imaged by the waveguide walls. The waveguide is thus seen to accurately simulate the waves in a plasma of infinite cross section. So far, only the case of a gradually increasing plasma density has been considered. If the change in plasma density per wavelength is more rapid, reflection due to impedance mismatch will result as well as refraction of the transmitted portion of the wave. The transmitted portion can be treated in the same manner as just discussed with account being taken of the reflection loss as an additional attenuation of the forward wave. The reflected wave increments from each incremental length of the plasma will themselves be TE_{10} mode waves made up of pairs of TEM waves in the same manner as the forward wave. The resultant reflected wave at the waveguide input would then be the vector sum of all the reflected wave increments and could be determined by integrating the expression for the reflected wave per unit length with phase referred to the waveguide input.

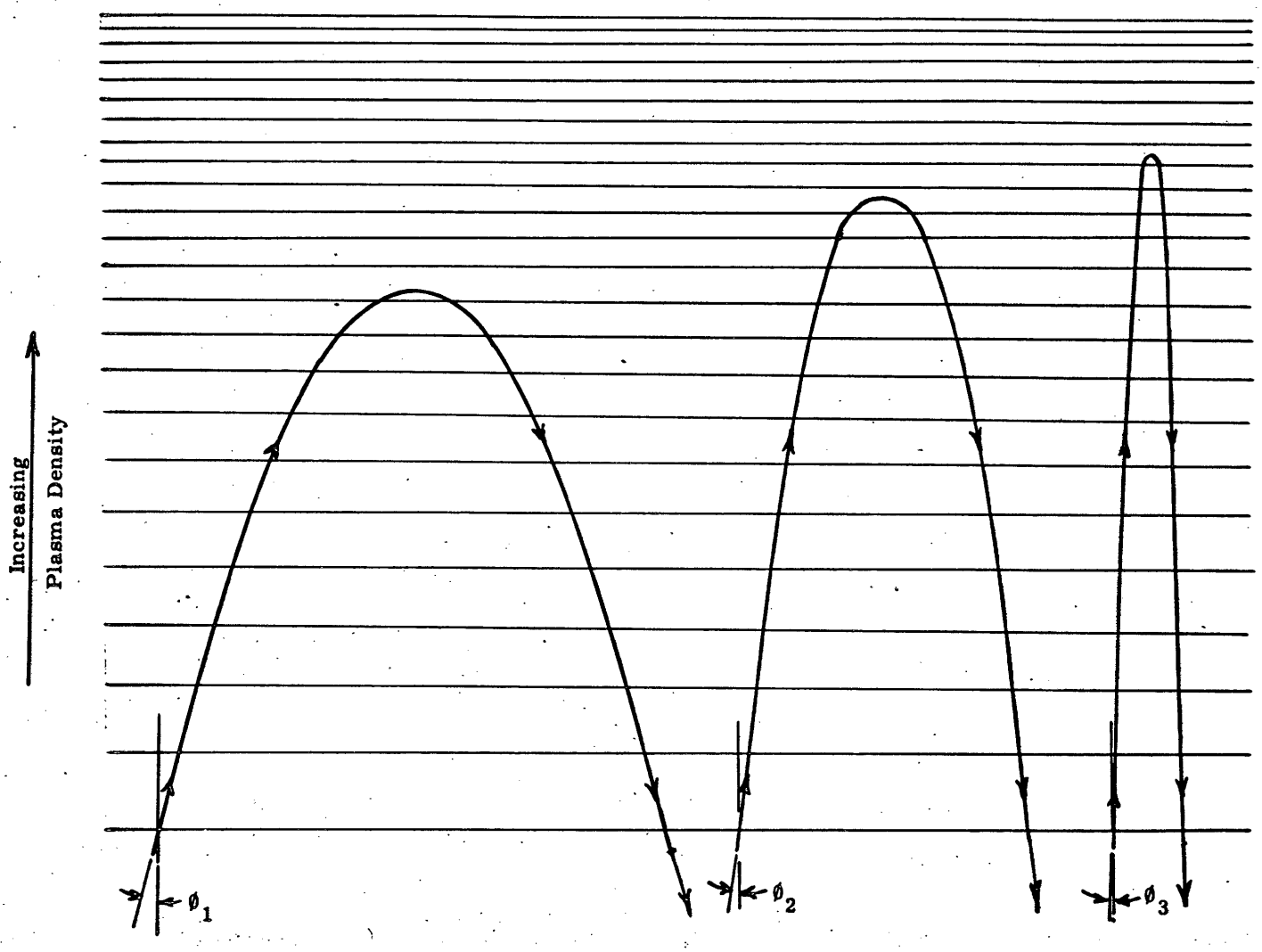

REFRACTION BY REGION OF INCREASING PLASMA DENSITY FOR THREE ANGLES OF INCIDENCE

FIG.20

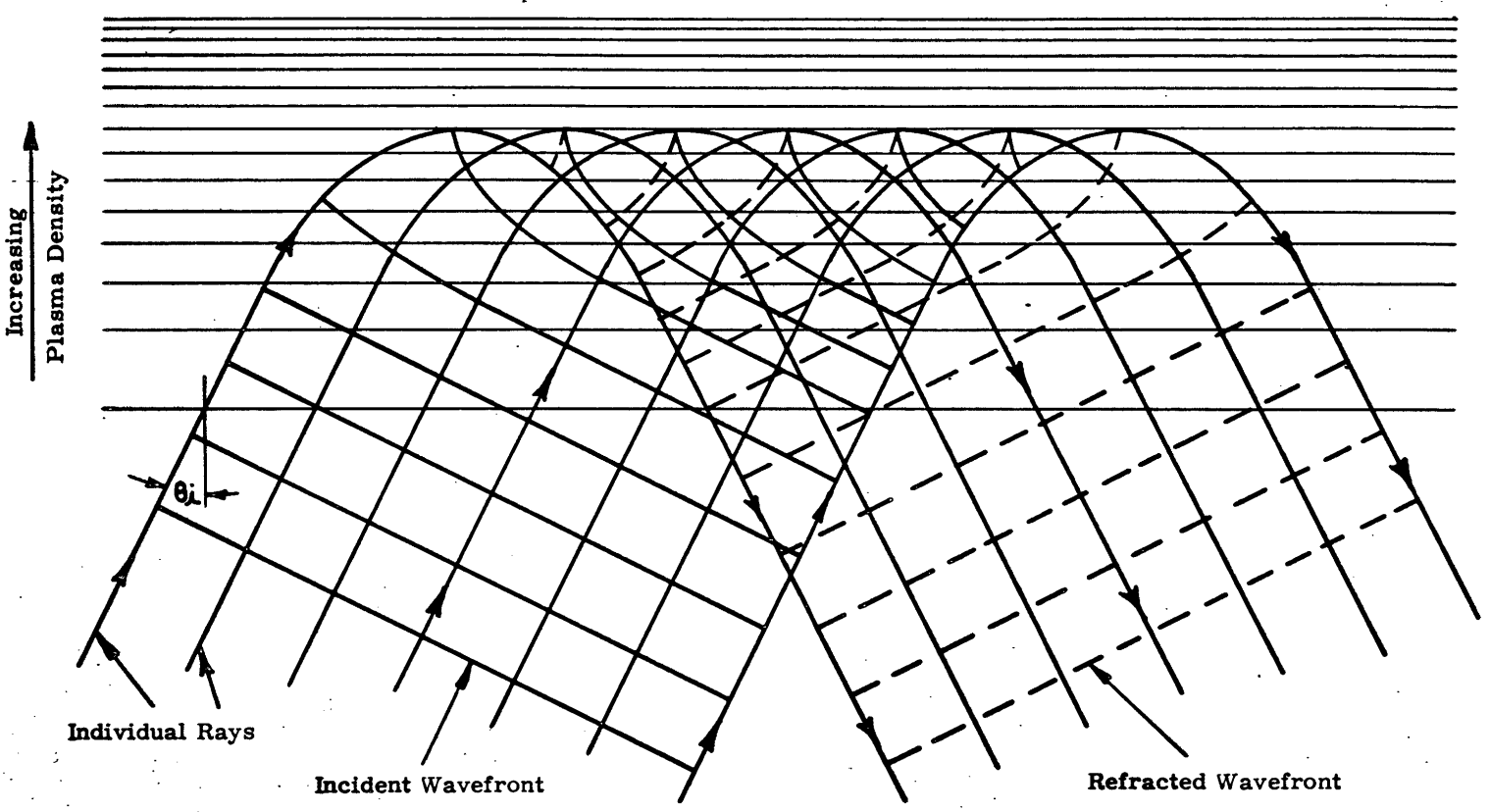

WAVE REFRACTED BY REGION OF INCREASING PLASMA DENSITY

FIG. 21

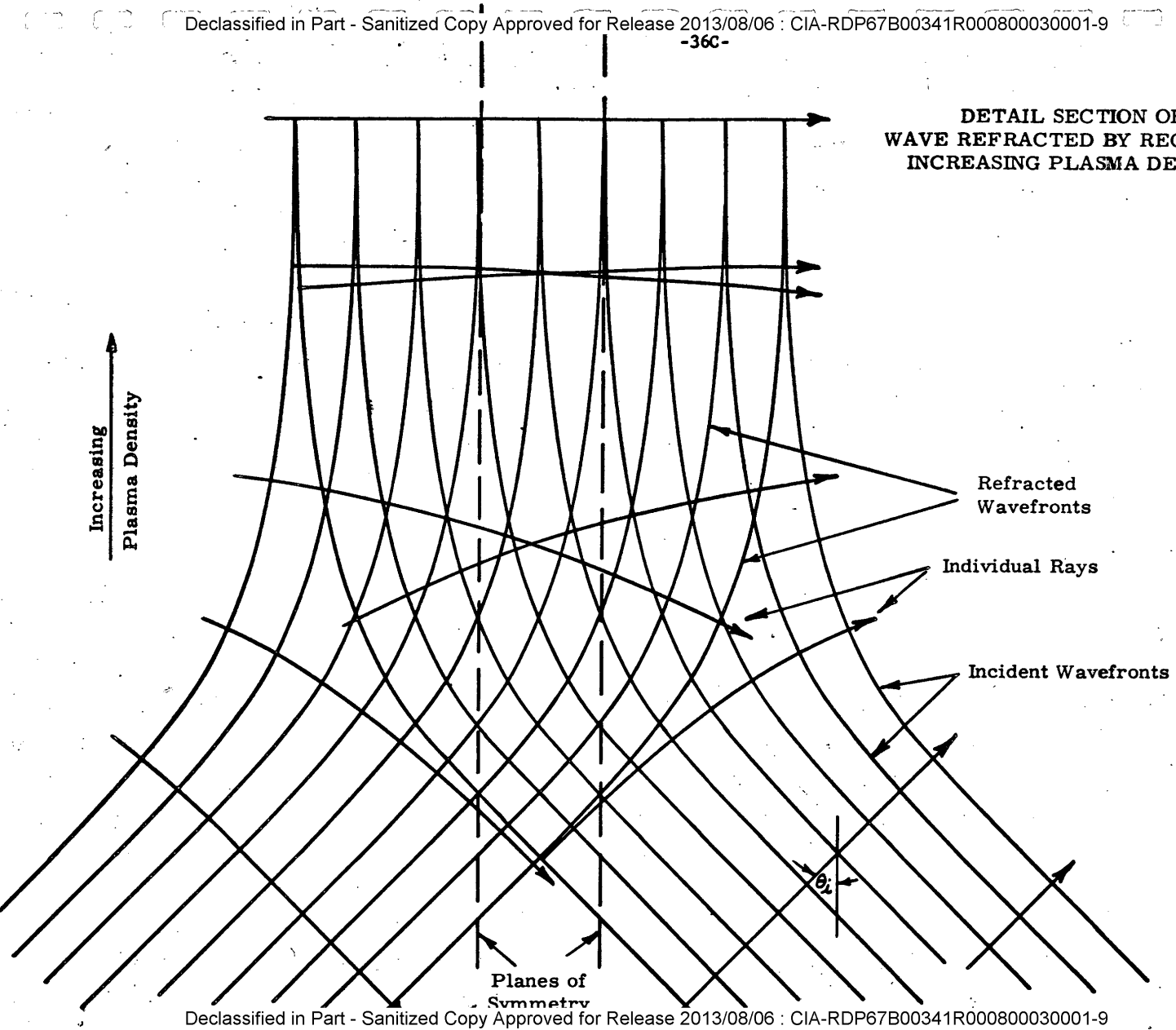

FIG. 22

COMPONENT WAVES IN WAVEGUIDES FILLED WITH PLASMAS OF DIFFERENT DENSITIES

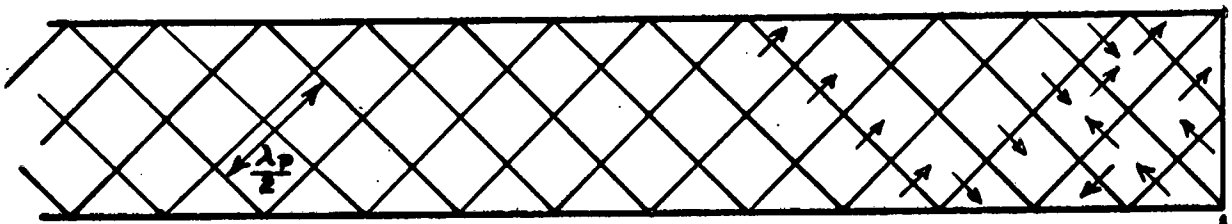

(a) Uniform Plasma - $\phi_i = 45^\circ$

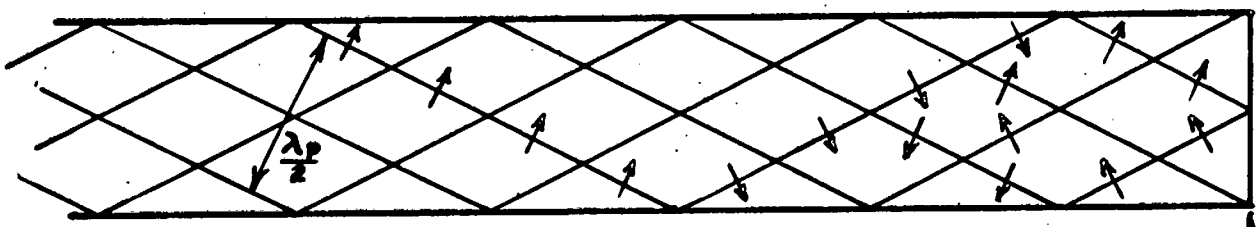

(b) Uniform Plasma - $\phi_i = 63.4^\circ$

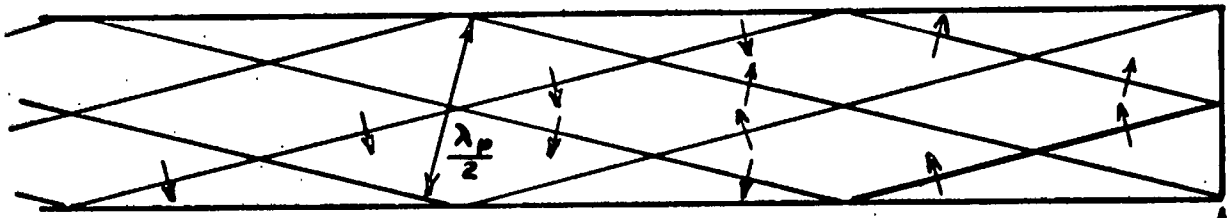

(c) Uniform Plasma - $\phi_i = 76^\circ$

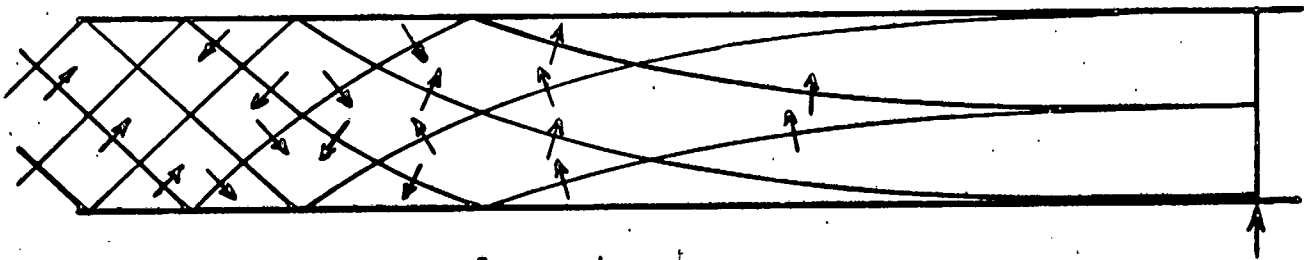

(d) Increasing Plasma Density →

FIG. 23

VI. WALL EFFECTS - REFLECTION OF PRIMARY ELECTRONS

An experiment was conducted to determine the effects that the wave guide walls might have on the electron density. Probe measurements, as described elsewhere in this report, have shown that the walls of the waveguide do not represent an important electron sink as the electron density across the guide is relatively constant, falling sharply only within an inch or so of the walls. Concern was expressed, however, that reflection of primary electrons off the walls might give a much higher electron density relative to the power of the primary beam than could be obtained under free space conditions. Figure 24 illustrates the problem.

An unconfined plasma would take on the more or less hemispherical shape shown by the dotted line in Figure 24. Under equilibrium conditions this must be accomplished by a net outward flow of electrons across the lines marking the waveguide walls. With the waveguide in place, however, some of the primary electrons that would normally cross the waveguide walls will be absorbed by the walls, but others will be reflected. If the reflected energy is appreciable, a given beam power could result in a much higher primary electron intensity, and therefore secondary electron density, within the waveguide than would exist in that same volume under free space conditions.

Figure 25 shows the relationship between the angle of incidence of the primary electron and the number and energy of the reflected electrons. Taking the worst possible case, if the energy dissipation from the primary electrons were distributed evenly throughout the volume occupied by a hemisphere 8 feet in radius, the total volume of the plasma cloud would be 1070 cubic feet. On the other hand, the volume occupied by the plasma in the waveguide is only 49 cubic feet.

We do not have the energy reflection coefficient for electrons at 20 KeV. In the range of 125 KeV to 2 Mev however, there is little change in the value of the coefficient from the values shown in Figure 25, so for the purposes of the present argument, we will assume the average value of Figure 25, namely 0.2255.

These numbers indicate that 95.4% of the energy in the electron beam would flow out into a volume that is not accessible to it when it is confined in the waveguide. Since it appears reasonable to assume that the primary electrons are travelling in all directions by the time they hit the wall, we can say that 95.4% of the energy of the primary beam is reflected back into the waveguide with an average efficiency of 22.55%. On this basis, the energy reflected back into the waveguide is about 21.5% compared with 4.6% that would normally be dissipated in the guide. Thus, by means of this crude analysis, it would appear that the plasma density in the waveguide for a given electron beam power might be as much as 4 or 5 times larger than would be expected in free space.

Since this confinement effect should become more severe the more the plasma is confined, an experimental evaluation of the effect was made by placing an eight-inch diameter aluminum pipe inside the waveguide with its axis coincident with the axis of one of the electron beams. A small slot was cut in opposite sides of the pipe for a length of about 6 inches in order that a probe could be passed through the pipe, thus enabling us to make measurements of the electron density inside and outside the pipe during the same run and with the same probe. Figures 26 and 27 show the results of these tests.

We conclude that the wall effect is not significant, at least with 20 kv electrons. In our crude analysis we made the simplifying assumption that the energy dissipation of the primary beam, and therefore the plasma density, was uniform throughout the volume of the hemispherical cloud. That this is not true can be seen from Figure 28. Although the contours of Figure 28 are for 400 keV electrons in air at 760 mm of mercury pressure, visual observations show that the shape of the contours is not significantly different at other pressures or other primary beam energies. Figure 28 indicates that the energy dissipation distribution is far from uniform, but is concentrated very sharply in a relatively small volume near the gun. This portion of the beam is not confined by the walls and the effect of the walls is thus reduced considerably from that predicted by our rough analysis.

Figures 26 and 27 show that inside the pipe the electron density peaks rather sharply, thus giving a larger diffusion loss of the plasma electrons than occurs in the waveguide itself. This effect undoubtedly compensates for the effect of at least part of the reflected primary electrons.

The effect of confining the plasma is not of significance in most of the tests that are reported and discussed in this report. The primary significance lies in the experiment that will be run using the 35-foot wave guide and the 150 kv electron gun. Here the volume enclosed by the waveguide is only about 1/2 of one percent of the volume of the hemisphere of the unconfined plasma, and significant primary electron reflection could render meaningless all attempts to estimate the power required in the ultimate application. A preliminary analysis, which is based on the fact that the primary electron beam energy dissipation is not uniform, shows that confinement of the beam by the waveguide at 150 kv may give an electron density per unit of beam power that is high by a factor of about five. Further analysis of this case is required, and the results of this analysis will be reported separately at a later date.

Some consideration was given to methods of reducing the number and energy of the reflected electrons should this be necessary. There appear to be several ways this could be done, all of them involving the use of thin sections of aluminum. These thin sections would, in part, reduce the reflection coefficient by allowing some of the electrons to be transmitted through the aluminum, and in part would reduce the effective coefficient by trapping the electrons so that multiple reflections would be required before the electrons could find their way back into the waveguide.

These electron absorbers might take several forms. Aluminum foams are available that could be used, as are honeycomb structures which would provide the deep cavities required for multiple reflections. Thin foils, spaced away from the waveguide wall, should also be effective in reducing reflections through transmission of the primary electrons. At the moment, we do not feel that such steps are required because we feel that reflection will not be a serious problem. If a problem does exist, however, we feel that it can be reduced to acceptable levels through the methods described above.

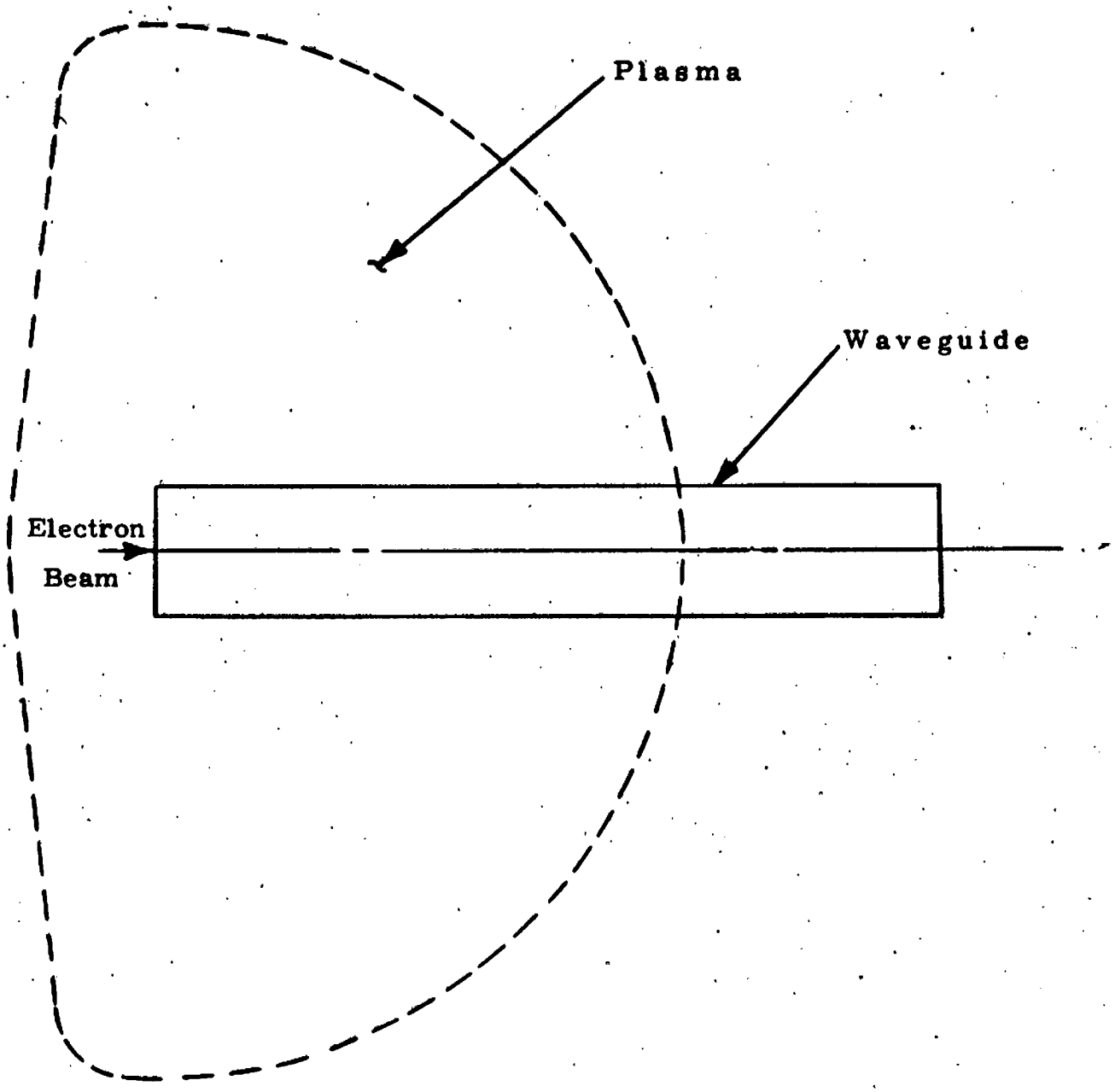

SKETCH SHOWING THE WAVEGUIDE
RELATIVE TO AN UNCONFINED PLASMA

FIGURE #24

Number and Energy Reflection Coefficients for 125 Kev Electrons

From: "Transmission & Reflection of Electrons by Aluminum Foils"

by Martin J. Berger

NBS Technical Note 187

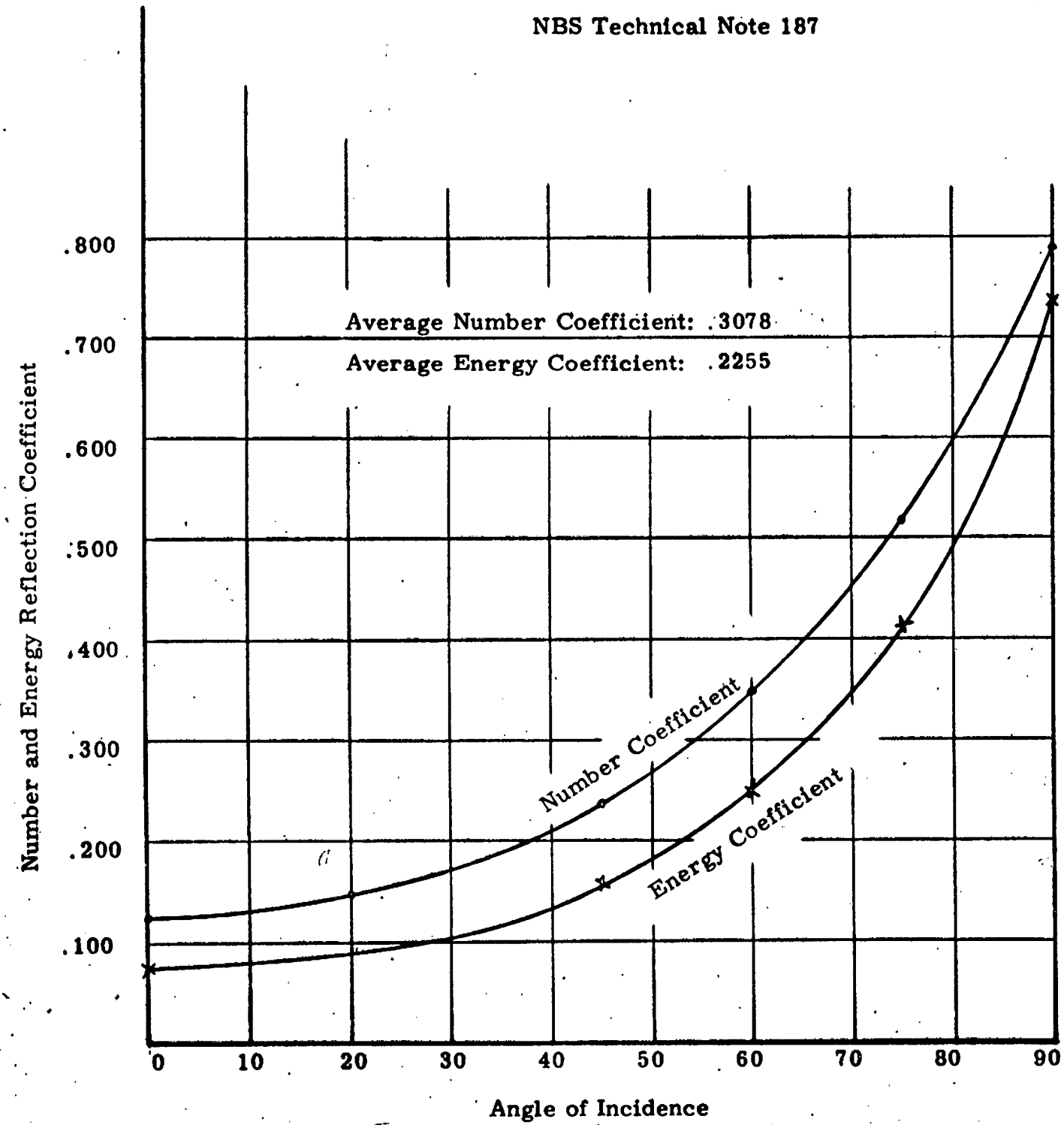

FIGURE #25

DISTRIBUTION OF Ne WITH DISTANCE ACROSS TANK AT 36" FROM ORIFICE WITH 8" PIPE IN PLACE

3 mm Air

1 ma Both Cups

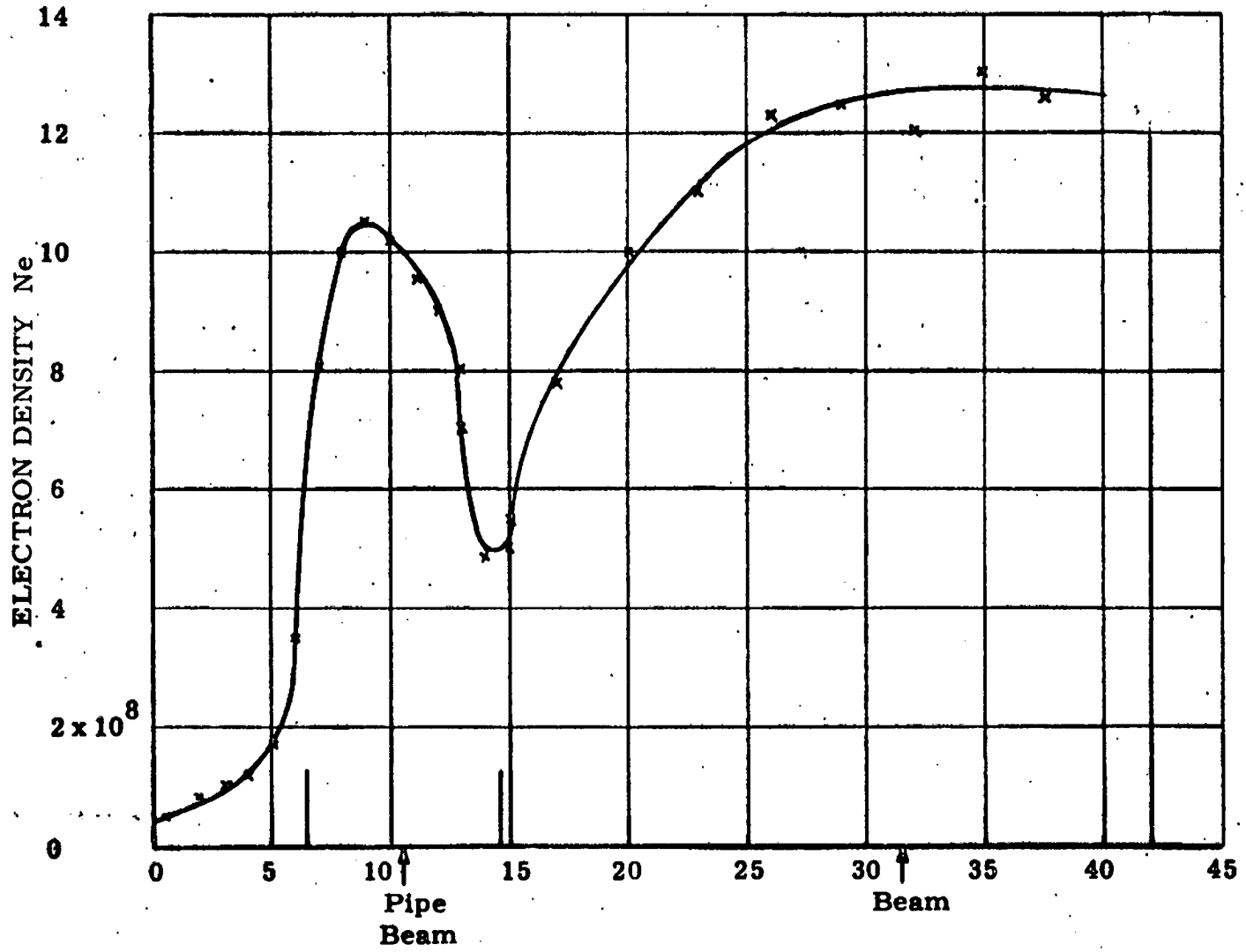

FIGURE #26

DISTRIBUTION OF Ne ACROSS TANK WITH PIPE IN PLACE

3.2 mm Air
10 ma on each Cup (Nominal)
Probe .001" x 3 cm Iridium

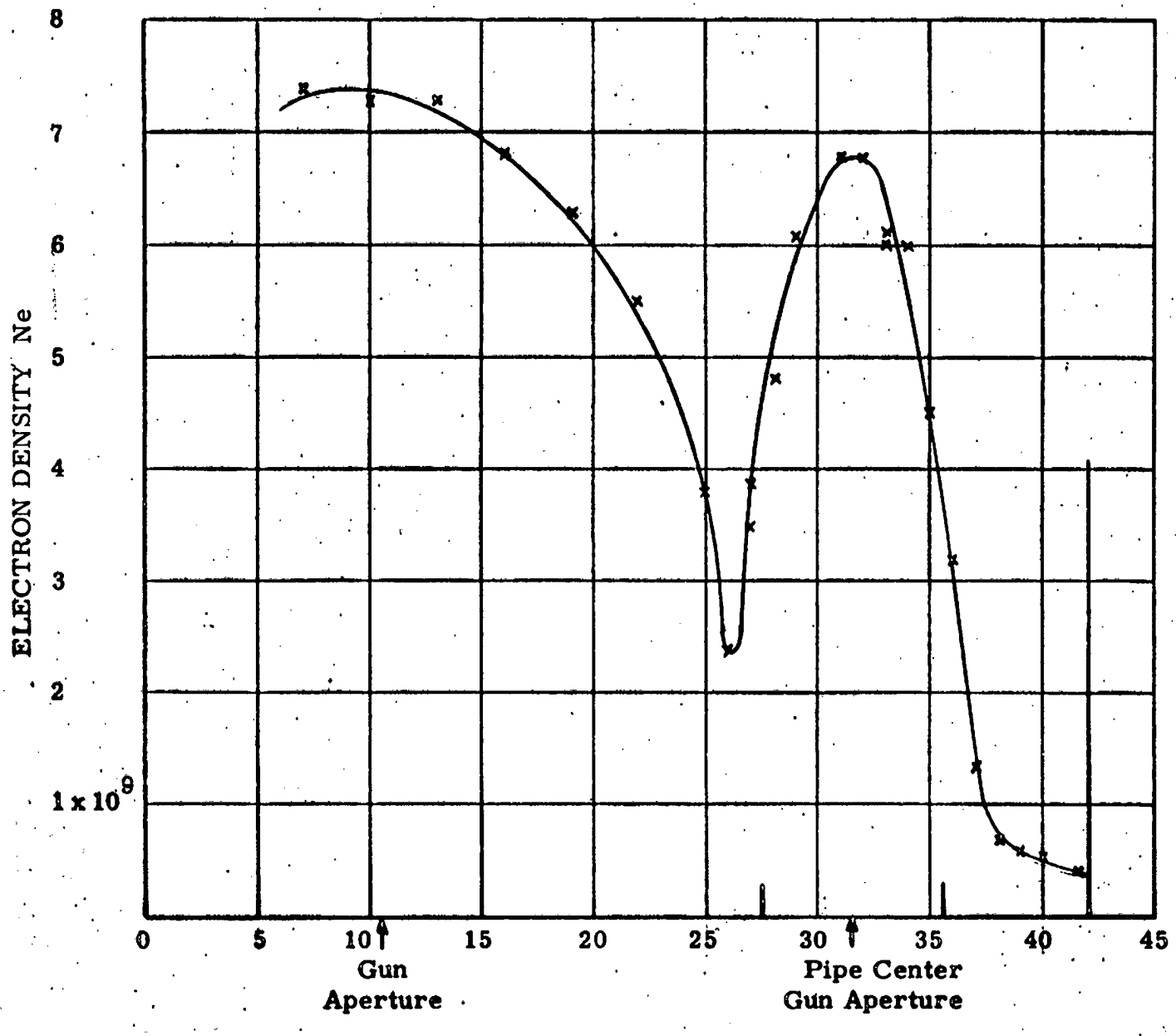

FIGURE #2[illegible]

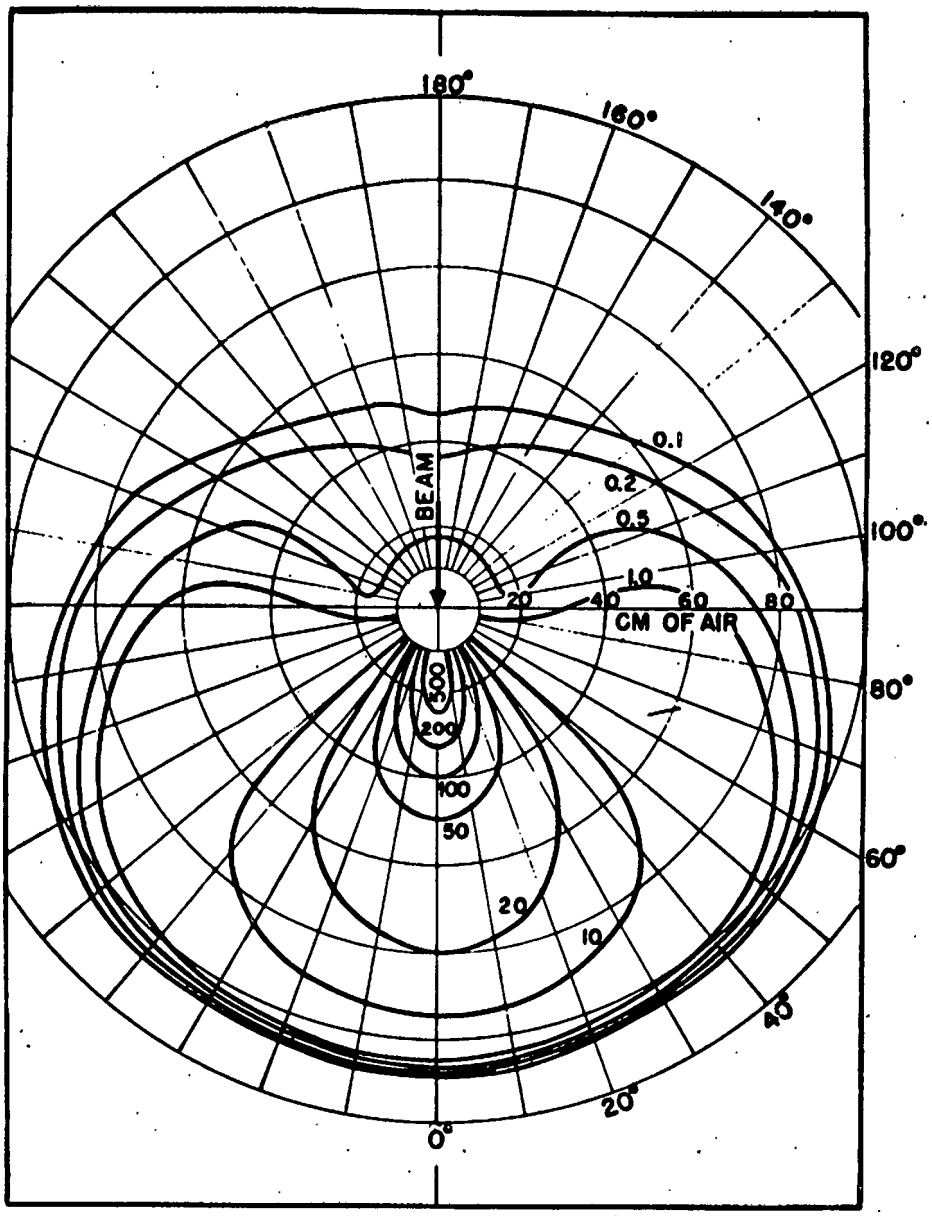

*

Contours of constant energy dissipation in air for 0.4 Mev electrons.

Figure #28

*Taken from: Jr. of Research of the National Bureau of Standards, by John E. Crew, Vol. 65A, No. 2, March-April 1961, pg. 116.

VII. HIGH PRESSURE PROBING

Langmuir probes generally give valid results only when the probe diameter is much less than the mean free path of the electrons. Already at 3 mm gas pressure where the mean free path is .006 inches, probe diameters not exceeding .001 inches are desirable. Mechanical considerations dictate that .001 inches is nearing the lower practical limit.

For these reasons a considerable effort was spent in evaluating other methods of probing designed to aid us in determining the electron density distribution in the forthcoming 150 KV experiment at 20 mm gas pressure.

Microwave interferometer experiments involving projecting a K band beam transversely across the waveguide and measuring the wavelength change were calculated to give a marginally low wavelength change for the relatively low densities in the order of 10^8 to 10^9 per cm^3 with which we will be concerned.

Attempts to measure the plasma conductivity or impedance between two plates or wires immersed in the plasma at various frequencies were tried and failed because of coupling problems to the waveguide cavity and difficulty of interpretation of the results.

It was therefore decided to run a set of measurements of electron densities as seen by probes of three different sizes placed close together in plasmas at different pressures. Then as the gas pressure is increased, the degree of fall off in apparent density seen by the larger probes can be determined, and by extrapolation a calibration for the 20 mm pressure can be obtained.

Time did not permit completion of this work, but sufficient data was obtained to indicate that a .0005" diameter probe, or even a .001" diameter probe will yield moderately accurate electron density data at 20 mm gas pressure. In these tests three probes of .002", .001" and .0005" diameter, respectively, were grouped near each other in plasmas at gas pressures of 3, 7, 10, 15 and 20 mm, and then the indicated plasma density was deduced for each pressure and probe size. There was a

considerable spread in the data of a random type for reasons which could not be determined in the time available, but there was no indication of a trend of steady reduction in apparent density as seen by the two larger probes as compared to the smaller probe as the pressure was increased.

More work should be done on this problem if accurate results are to be assured.

PROJECT 522 - Task V

View of equipment with pair of PEB guns in right foreground.

PROJECT 522 - Task V

View through side window showing beam entering waveguide from exit aperture.

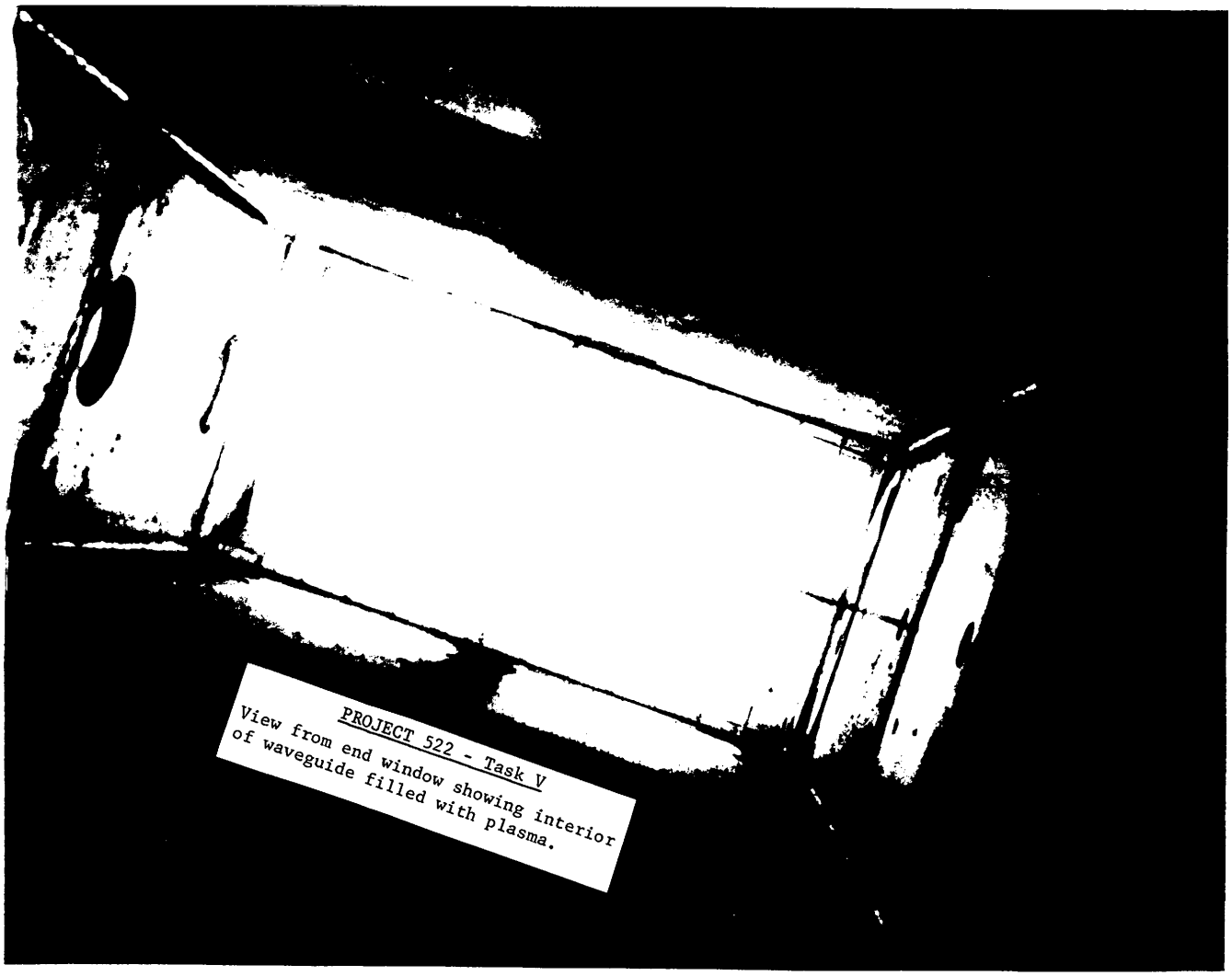

PROJECT 522 - Task V
View from end window showing interior of waveguide filled with plasma.